THE OCCURRENCE OF VERTEBRATE AND INVERTEBRATE FOSSILS IN A SEQUENCE STRATIGRAPHIC CONTEXT: THE JURASSIC SUNDANCE FORMATION, BIGHORN BASIN, WYOMING, U.S.A

Author(s): SHARON K. MCMULLEN, STEVEN M. HOLLAND, and F. ROBIN O'KEEFE
Source: PALAIOS, 29(6):277-294. 2014.
Published By: Society for Sedimentary Geology
URL: http://www.bioone.org/doi/full/10.2110/pal.2013.132

PALAIOS
Emphasizing the impact of life on Earth's history

PALAIOS, 2014, v. 29, 277–294
Research Article
DOI: http://dx.doi.org/10.2110/pal.2013.132

THE OCCURRENCE OF VERTEBRATE AND INVERTEBRATE FOSSILS IN A SEQUENCE STRATIGRAPHIC CONTEXT: THE JURASSIC SUNDANCE FORMATION, BIGHORN BASIN, WYOMING, U.S.A.

SHARON K. MCMULLEN,[1] STEVEN M. HOLLAND,[1] AND F. ROBIN O'KEEFE[2]
[1]University of Georgia, Department of Geology, Athens, Georgia, 30602-2501, U.S.A., skmcmull@gmail.com, stratum@uga.edu
[2]Department of Biological Sciences, Marshall University, Huntington, West Virginia 25755, U.S.A., okeefef@marshall.edu
e-mail: stratum@uga.edu

ABSTRACT: **Previous studies of the sequence stratigraphic distribution of fossils have focused on the record of relatively abundant marine invertebrates. Only a handful of studies have examined how sequence stratigraphic architecture influences the occurrence of vertebrates, particularly large and rare tetrapods. The Jurassic Sundance Formation of the Bighorn Basin, Wyoming, USA, contains a rich suite of invertebrate and vertebrate fossils, including large and rare marine reptiles, and this allows the sequence stratigraphic controls on the distribution of these groups to be compared. The Sundance Formation consists of four depositional sequences, with the lower two being carbonate dominated and the upper two siliciclastic dominated. Two incised valley fills are also present. The presence of multiple depositional sequences and strongly erosional sequence boundaries is the likely cause of the complicated lithostratigraphic nomenclature of the Sundance. Invertebrates (mollusks and echinoderms) in the Sundance conform to well-established patterns of occurrences, including strong facies control and fossil concentrations at maximum flooding surfaces, in the upper portion of parasequences, and within lags overlying sequence boundaries. As expected from their rarity, marine reptiles (ichthyosaurs, plesiosaurs, and pliosaurs) show a weaker connection to sequence stratigraphic architecture. Nonetheless, they do display facies control and are found primarily in offshore mudstone, rather than shoreface and estuarine sandstone. They are also more common at hiatal surfaces, including a zone of concretions at the maximum flooding surface and in lag deposits overlying sequence boundaries. These associations suggest that sequence stratigraphic architecture may be a useful approach for discovery of marine vertebrates and that sequence stratigraphic context should be considered when making paleobiological interpretations of marine vertebrates as well as invertebrates.**

INTRODUCTION

Numerous field and modeling studies over the past twenty years have documented the close correspondence between the fossil record and sequence stratigraphic architecture, but nearly all of this research has focused on the rich invertebrate fossil record (Brett 1995; Holland 1995, 2000; Kidwell 1991; Patzkowsky and Holland 2012). In particular, these studies have documented sequence stratigraphic control on the occurrence of shell beds, as well as on changes in abundance, community structure, and morphology. Far fewer studies have focused on vertebrates, owing to their rarity; however, these few studies have also recognized sequence stratigraphic control on the occurrence of vertebrate fossils (Rogers and Kidwell 2000; Eberth et al. 2001; Allulee and Holland 2005; Peters et al. 2009; Loughney et al. 2011). Because marine vertebrate fossils differ from invertebrates in size, abundance, durability, and composition (Peters et al. 2009), a better understanding of how these differences affect preservation and stratigraphic distribution is needed. Understanding these controls would not only improve paleobiological and biostratigraphic interpretations (Loughney et al. 2011), it could also facilitate the discovery of these rare fossils.

The Middle Jurassic Sundance Formation of the western United States is an ideal setting to contrast sequence stratigraphic controls on vertebrate and invertebrate fossils because of its diverse and abundant fauna (Massare et al. 2014). Vertebrate fossils in this unit are dominated by one species of ichthyosaur (Massare 2004; Wahl 2009), but also include two cryptocleidoid plesiosaurs (Street and O'Keefe 2010; Wilhelm and O'Keefe 2010; O'Keefe et al. 2011) and a pliosaur (Wahl et al. 2007), as well as chondrichthyans (Wahl 1998) and teleosts (Schultze and Enciso 1983). Invertebrates include bivalves, gastropods, belemnites, ammonoids, serpulid worms, malacostracans, insects, ostracods, crinoids, asteroids, and echinoids (Imlay 1948, 1957, 1980; Swain and Peterson 1952; Peterson 1954; Wright 1973, 1974; Herrick and Schram 1978; Blake 1981; Kvale et al. 2001; Santiago-Blay et al. 2001; Palmer et al. 2004; Hunter and Zonneveld 2008; Wahl 2008). This study presents a sequence stratigraphic interpretation of the Sundance Formation in the Bighorn Basin of north-central Wyoming, and uses it to infer the sequence stratigraphic controls on the occurrence of vertebrate and invertebrate fossils.

GEOLOGIC CONTEXT

Stratigraphic Relationships

The Bathonian to Oxfordian (168–157 Ma) Sundance Formation is approximately 100 m thick and records cyclic deposition in a mixed siliciclastic-carbonate system. The Sundance occurs over a broad region stretching from South Dakota to Idaho and from Colorado to Montana (Parcell and Williams 2005), and it is particularly well exposed in hogbacks on the western slopes of the Bighorn Mountains (Fig. 1). The Sundance Formation overlies the Bajocian Gypsum Spring Formation and Piper Formation, which includes facies interpreted as shallow marine

Published Online: September 2014
 0883-1351/14/029-277/$03.00

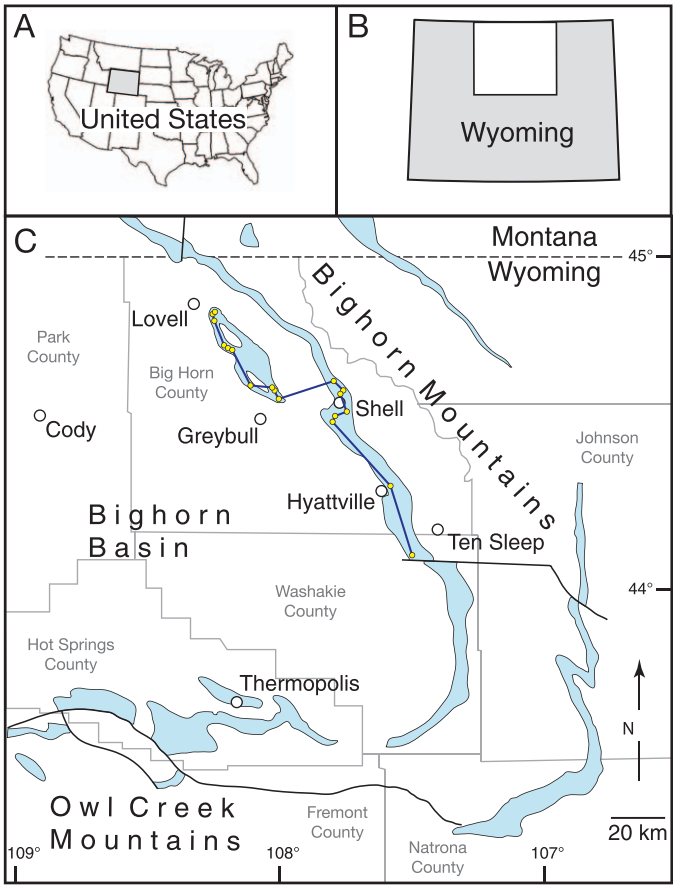

FIG. 1.—Location map of study area. **A**) United States. **B**) Wyoming with outline of locality area. **C**) Localities in study shown with yellow dots. Outcrop area of Jurassic strata shown in blue. Cross section A–A′ of Figure 6 indicated by blue line.

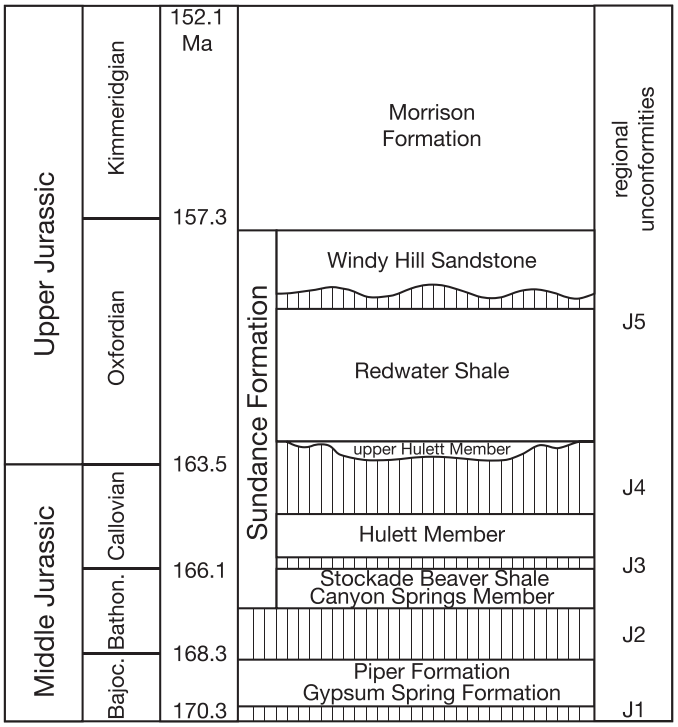

FIG. 2.—Chronostratigraphic and lithostratigraphic framework of the Sundance Formation and adjacent units in the Bighorn Basin of Wyoming, with age relationships based on Imlay (1982), Calloman (1982), Kvale et al. (2001), and Massare et al. (2014). Unconformities recognized by Pipiringos (1968) and Pipiringos and O'Sullivan (1978) are shown at right. The durations of the J2 and J4 are based on Imlay (1982), but the durations of the J3 and J5 are inferred. Absolute time scale is from Cohen et al. (2013).

to tidal flat and sabkha (Fig. 2). The Sundance Formation is overlain by the terrestrial deposits of the Late Jurassic (148–155 Ma) Morrison Formation (Imlay 1962, 1980; Pipiringos 1968; Kowallis et al. 1998). Evidence for the age of the Sundance and its members is summarized by Calloman (1982) and Kvale et al. (2001). Regional unconformities J1–J4, recognized largely based on the presence of chert-pebble horizons, have been correlated into the Bighorn Basin, although the position of the J3 unconformity is uncertain (Pipiringos 1968; Pipiringos and O'Sullivan 1978; Schmude 2000; Kvale et al. 2001). Although regional syntheses of the Sundance Formation and correlative units have been conducted previously, most predate sequence stratigraphic concepts and make extensive use of offshore bars and barrier islands to explain complex facies relationships (e.g., Brenner and Davies 1974; Rautman 1978).

The complex intertonguing of the mudstone, limestone, and sandstone in the Sundance Formation has fostered a complex lithostratigraphic nomenclature (Fig. 2; Imlay 1947, 1980; Pipiringos 1968; Wright 1973; West 1985; Kvale et al. 2001). In some areas, up to seven members have been described (Pipiringos 1968). In the Bighorn Basin, the Sundance Formation is divided into informal upper and lower units (Imlay 1956; Wright 1973; Rautman 1978). This lower Sundance includes, from bottom to top, the Canyon Springs Member, the Stockade Beaver Shale, and the Hulett Member (Imlay 1956; Schmude 2000). The upper Sundance consists primarily of the Redwater Shale, capped by the hogback-forming Windy Hill Sandstone (Imlay 1957; Pipiringos 1968). Because of its gradational contact with the overlying Morrison Formation, the Windy Hill Sandstone has been included by some as a member of the Morrison (Peterson 1994).

Paleogeography and Tectonic Setting

From the Bathonian to the Oxfordian, the Sundance Seaway extended as shallow epeiric sea a remarkable 2000 km southward from its connection to the open ocean near the southern border between the Yukon Territory and Northwest Territories of Canada (Blakey 2013). This narrow seaway was bounded to the west by a volcanic arc, to the east by the North American craton, and to the south by a prograding coastal plain draining from the Ancestral Rockies (Fig. 3; Imlay 1957; West 1985; Peterson 1994; Kvale et al. 2001). Recent paleogeographic reconstructions place Wyoming at 35° to 40°N during the Middle Jurassic (Blakey 2013), with a slow northward drift, although older reconstructions place Wyoming in a more southerly position, at 22° to 33°N (e.g., Kocurek and Dott 1983). Previous sedimentologic studies indicate that the Sundance Formation records deposition in a variety of environments, including shallow shelf (Wright 1973; Brenner and Davies 1974; DeJarnette and Utgaard 1986; Parcell and Williams 2005), tidal flat (Kvale et al. 2001), eolian (Stone and Vondra 1972; Kilibarda and Loope 1997), and estuarine (Uhlir et al. 1988).

In shape and areal dimensions, the Sundance Seaway was comparable to the modern Red Sea, but with a widened terminus; however, the shallow marine facies and the thinness of the Sundance Formation indicate that the Sundance Sea was far shallower. This configuration in this paleogeographic setting would likely have had several significant effects (Kocurek and Dott 1983; Peterson 1994). A 30°–40°N

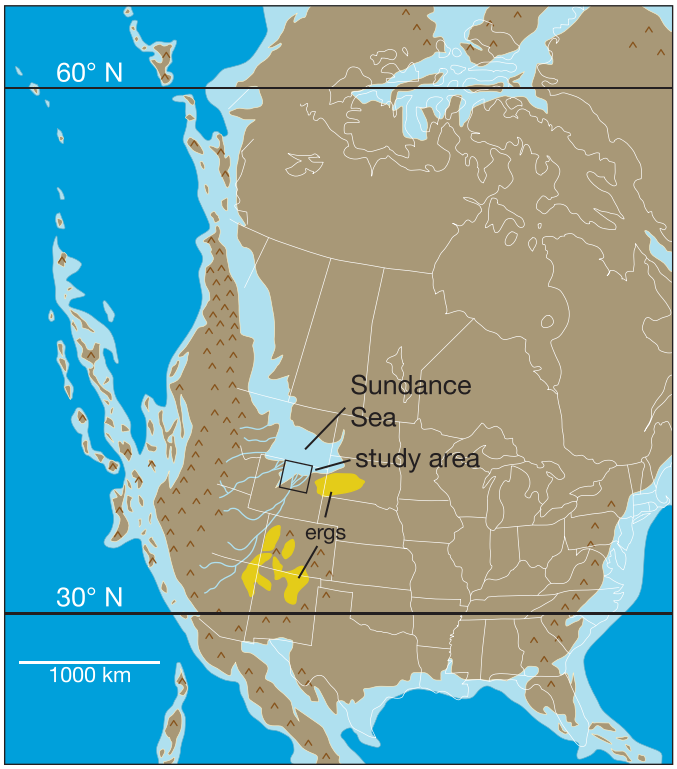

FIG. 3.—Paleogeographic reconstruction of the Sundance Seaway, adapted from the Late Jurassic map of North America by Blakey (2013).

paleolatitude likely would have led to prevailing winds from the west, with the Bighorn Basin lying in an arid zone when at the southern end of these paleolatitudes and in a humid, temperate zone when at the northern end of these paleolatitudes. In this scenario, with a volcanic arc to the west, prevailing winds would likely have generated a rain shadow over the region. The orientation of the seaway perpendicular to the prevailing winds would likely have also limited the fetch for waves. The interior position of the seaway behind a volcanic arc, and its position on the western side of the continent would have isolated the region from most tropical storms. The extraordinary length of such a shallow and narrow seaway would likely have limited substantial tidal exchange and may have allowed marked departures in salinity from normal marine conditions. When the southern terminus of the seaway lay within an arid belt (cf. Kocurek and Dott 1983; Peterson 1994; Kvale et al. 2001), hypersaline conditions may have occurred, but when the terminus was within a more northerly and temperate zone, brackish conditions would have been more likely.

The Sundance Seaway lay in a retroarc position behind the volcanic arc to the west, but the cause of subsidence within this basin has been intensely debated (DeCelles 2004; Fuentes et al. 2009; Miall 2009). Although the Sundance and Morrison Formations and their age equivalents in Montana have been thought to have been deposited within a retroarc foreland basin, they do not thicken westward toward the fold and thrust belt (Heller et al. 1986). More recently, the region has been interpreted as the back-bulge region of a retroarc foreland basin (DeCelles and Currie 1996), but the lack of any Jurassic foredeep sediments to the west would require the complete erosion of the entire foredeep succession (DeCelles 2004). Recent subsidence, petrographic, and detrital zircon evidence from Montana suggest a Late Jurassic initiation of the Western Interior foreland basin, with the Sundance having been deposited within a back-bulge basin (Fuentes et al. 2009). Because both types of basins are dominated by flexural subsidence, the differences between them are unlikely to have a significant effect on sequence stratigraphic architecture in the Bighorn Basin.

METHODS

Field Data

Eighteen stratigraphic columns of the Sundance Formation were measured along an approximately 240 km northwest to southeast transect on the eastern flank of the Bighorn Basin (Fig. 1). Localities were targeted to include sites where vertebrate fossils had been found previously. Coordinates of columns are provided in the Appendix (also see online Supplementary Data File).

At each column, beds were described for physical sedimentary structures, color, lithology, grain size and angularity, sorting, continuity, thickness, diagenetic minerals, bioturbation, ichnofossils, and body fossils. Twenty thin sections were prepared to characterize lithology. Bedding thickness is reported with the Ingram (1954) scale, siliciclastic rock names follow Pettijohn et al. (1987), and carbonate rock names follow Dunham (1962).

A total of 185 faunal censuses of invertebrate (online Supplementary Data File) and vertebrate fossils were conducted in the field on bedding planes and weathered shale surfaces of 1–2 square meters. Faunal censuses were performed for 15–20 minutes each to provide a consistent sampling effort. Faunal abundance of each species was recorded as rare (1–2 specimens), common (3–10 specimens), abundant (10–20 specimens), or very abundant (>20 specimens). Voucher specimens were collected for identification.

Quantitative Paleoecology

Ordination analysis was used to identify and describe faunal gradients in the fossil data, and to determine any associations between fossil assemblages and lithofacies. Prior to ordination, species that occurred in only one sample and samples that contained only one species were removed, because they provide no information on faunal gradients. This culling reduced the number of samples from 53. Following this culling, the Wisconsin double standardization transformation was applied to correct for variations in sample size and species abundance. Data were ordinated with Nonmetric Multidimensional Scaling (NMS), using the metaMDS function in the vegan package of the open source statistical software R (R Development Core Team 2011). Because NMS is a numerical rather than analytic ordination technique, twenty random restarts were used to avoid solutions that represent local minima (Legendre and Legendre 1998; McCune and Grace 2002).

Well Logs

Spontaneous potential (SP) logs from boreholes were obtained from the Wyoming Oil and Gas Conservation Commission and were used to correlate divisions of the Sundance Formation in the subsurface along the eastern flank of the Bighorn Basin. Comparison of well logs to nearby outcrops was used to establish the interpretation of the well-log signatures.

SUNDANCE FACIES ASSOCIATIONS

The Sundance Formation contains three facies associations. The lower Sundance is dominated by a carbonate ramp facies association (C), and the upper Sundance is dominated by the wave-dominated shelf (S) and tidal estuary (T) facies associations.

TABLE 1.—*Carbonate Ramp Facies Association C.*

Facies	Sedimentology	Paleontology	Geometry and contact relationships
C1—offshore	Bioturbated gray to tan sandy terrigenous and calcareous mudstone to siltstone, with pelleted texture and lacking in sedimentary structures. Small (0.5 cm) pyrite nodules, minor quartz silt and very fine sand.	Highly abundant *Gryphaea nebrascensis*, with diverse microfossils, including benthic foraminifera, ostracods, echinoid spines, and rare neoselachian shark teeth. Trace fossils: *Planolites*.	Tabular bodies 5–30 m thick. Always sharply overlain by other facies (e.g., S1, I2, C5, C2, C4).
C2—shallow subtidal	Interbedded sandy terrigenous mudstone to siltstone (similar to C1) and 10–50 cm thick beds of white, bioturbated skeletal/peloidal/ooidal wackestone to packstone. Limestone beds thicken upwards, as does number of ooids. Bioturbation generally intense and ripple lamination is rare. Fine to very fine quartz and chert grains common increase in abundance upwards, as do ooids. Includes 20–30 cm intervals of wave-rippled fine carbonate sand.	Common bivalves (*Myopholas*, few *Liostrea*), mostly as internal molds. Common isolated crinoid columnals (*Chariocrinus*). Gastropod internal molds locally common (e.g., *Lyosoma*), as are udoteacean algae, foraminifera, and ostracods. Spongiostromate pisoidal and oncoidal coatings common.	Tabular bodies 0.5 to 5 m thick. Sharply overlies maroon mudstone of Piper Formation at base of Sundance Formation. Locally gradationally overlain by Facies C3, but more typically sharply overlain by Facies C1.
C3—ooid shoal	Oolitic quartzose grainstone, often bearing highly fragmented skeletal grains. Ooids commonly micritized. Skeletal grains and pyrite nodules (0.5 cm) locally present. Quartz silt to lower very fine sand locally common. Trough cross-stratification, ripple-laminated, and planar laminated. Internal erosional surfaces with up to 2 m of relief, overlain by upward-thinning beds.	Bivalves, crinoid ossicles, foraminifera, and rare gastropods.	Tabular bodies approximately 1–2 m thick. Locally grades upwards rapidly into facies C5.
C4—lagoonal	Planar-laminated gray lime mudstone, locally with flaser to lenticular lamination. Contains abundant fine-grained quartz sand.	Insects, ostracods, and fish have been reported (e.g., DeJarnette and Utgaard 1986), but generally lacks fossils.	Tabular bodies 5–12 m thick, restricted to northernmost portion of study area. Sharply overlies Facies C1 and is sharply overlain by Facies S1 and S2.
C5—eolian	Oolitic quartzose grainstone, with large-scale (> 3 m) tabular foresets and inversely graded pin-stripe laminae. Meniscus cement common. Highly abraded and fragmented skeletal grains, mostly bivalves, commonly neomorphosed. Locally abundant grains of quartz silt to lower very fine sand. Raindrop impressions locally preserved. Uppermost surface locally bears wave ripples.	Highly abraded minute bivalve fragments.	Lenticular bodies up to 12 m thick. Sharply overlain by Facies S1. Locally erosionally overlain by Facies I2 and I3.

Carbonate Ramp Facies Association C

The carbonate ramp facies association consists of five facies that represent offshore (C1), shallow subtidal (C2), ooid shoal (C3), lagoonal (C4), and eolian (C5) environments (descriptions summarized in Table 1).

Facies C1 records deposition on the distal portion of a carbonate ramp, based on its marine fauna, uniformly fine grain size, dominance of bioturbation over physical sedimentary structures, regional lateral extent, and its gradational contact with Facies C2. Facies C1 is represented primarily by the Stockade Beaver Shale, but is also present in the lower portion of the Canyon Springs Member.

Facies C2 was deposited on the inner portion of a carbonate ramp, one characterized by relatively quiet water, as indicated by the dominance of bioturbation over physical sedimentary structures. Facies C2 is distinguished from Facies C1 by the presence of beds of limestone encased in mudstone (Fig. 4A), which may indicate storms, although specific evidence of storm-generated waves or currents is lacking. The abundance of crinoid columnals, accompanied by common bivalves and gastropods, suggests relatively normal marine salinity, and the presence of codiacean algae suggests clear water free of suspended sediment. Facies C2 comprises most of the Canyon Springs Member, and limited portions of the lower Hulett Member (of DeJarnette and Utgaard 1986).

Facies C3 is transitional from Facies C2 and records deposition on shoals on the innermost portion of a carbonate ramp (Stone and Vondra 1972). The abundance of ooids, commonly micritized, suggests well-lit shallow-water conditions, and the abundance of trough cross-bedding, ripple lamination, and planar lamination indicates frequent reworking by currents and waves (Fig. 4B). A *Skolithos* ichnofacies also supports shallow-water deposition. Quartz grains likely represent eolian input, and an increase in these grains to the south suggests a source in that direction. Locally, the top of this facies is wave rippled and bears tridactyl dinosaur footprints, indicating deposition near the shoreline (Kvale et al. 2001). Facies C3 is present at the tops of meter-scale cycles in the Canyon Springs Member, and it also comprises part of the lower Hulett Member.

Facies C4 records deposition in a quiet-water hypersaline lagoon behind shoals, as indicated by its fine grain size, papery planar lamination (Fig. 4C), and lack of burrows. This facies is reported to contain a sparse fauna of well-preserved insects, fish (*Pholidophorus americanus*), and ostracods (Imlay 1965; DeJarnette and Utgaard 1986; Kilibarda and Loope 1997; Santiago-Blay et al. 2001), although this fauna of insects, fish, and ostracods was not encountered in this study. Quartz grains are interpreted as eolian in origin. Facies C4 comprises the middle Hulett Member (of DeJarnette and Utgaard 1986) and is limited to the northern portion of the study area (Schmude 2000).

Facies C5 represents carbonate eolian dunes, as indicated by inversely graded pinstripe laminae, tabular foresets several meters tall (Fig. 4D), meniscus vadose cement, and raindrop impressions (Kilibarda and Loope 1997). Where Facies C5 overlies Facies C3, abraded bivalve fragments are locally present at the toes of some foresets. In a few outcrops, erosional surfaces with up to 2 m relief and overlain by an upward-thinning series of beds likely represent tidal channels. Wave ripples at the top of this facies likely record reworking during transgression (Kilibarda and Loope

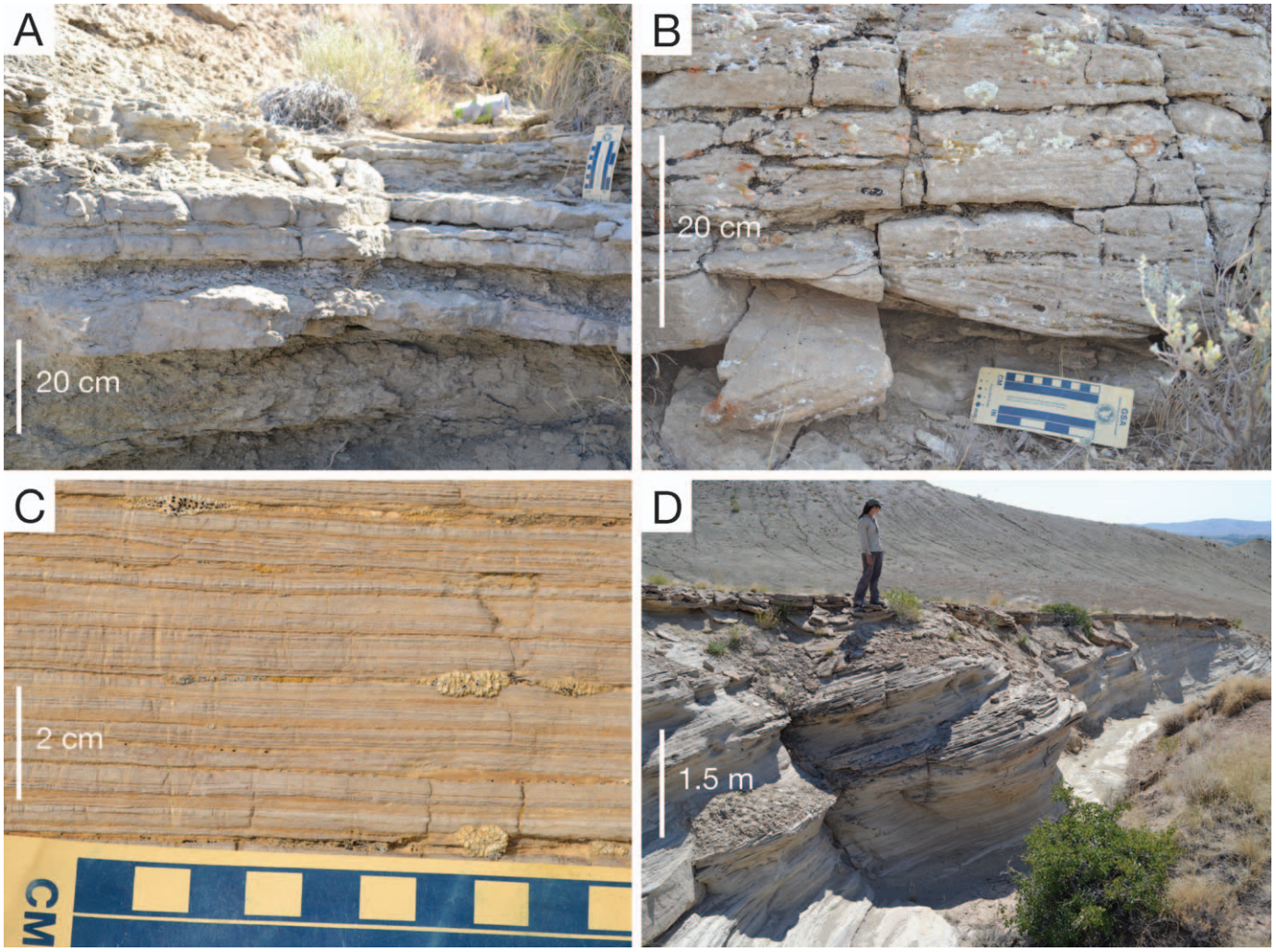

FIG. 4.—Carbonate ramp facies association. **A**) Facies C2, interpreted as shallow subtidal with beds of bioturbated skeletal/ooidal/peloidal wackestone and packstone interbedded with calcareous siliciclastic mudstone, and overlying Facies C1 (offshore). **B**) Facies C3, interpreted as ooid shoal, with cross-bedded ooid grainstone. **C**) Facies C4 (lagoonal), illustrating paper-thin planar laminae of lime mudstone. **D**) Facies C5 (eolian), displaying large-scale foresets, truncated at top by wave-ripple–laminated beds.

1997). Facies C5 comprises most of the lower Hulett Member in the central portion of the study area.

Overall the carbonate ramp facies association indicates deposition on a homoclinal ramp, much like those reported from other Jurassic settings (Burchette and Wright 1992; Aurell et al. 1995; Azeredo 1998). The abundance of ooids and the presence of large eolian dunes suggests semiarid to arid conditions during the Bathonian and Callovian. Paleocurrents on wave ripples indicate flow to the north-northwest and south-southeast, corresponding to a shoreline oriented west-southwest and east-northeast (Stone and Vondra 1972). Paleocurrent measurements on eolian foresets are more variable, but have dominant modes to the northwest and south-southwest (Stone and Vondra 1972).

Wave-Dominated Shelf Facies Association S

The wave-dominated shelf facies association consists of three facies that represent offshore (S1) and shoreface (S2) environments, as well as shell beds (S3) that occur at parasequence tops (Table 2). These three facies comprise the Redwater Shale of the upper Sundance.

Facies S1 represents relatively deep-water deposition on a siliciclastic shelf, as indicated by the fine grain size, marine fauna, *Cruziana* ichnofacies, and widespread geographic extent. Thin sandy to shelly beds likely reflect storm beds (Fig. 5A, Brenner and Davies 1973; Specht and Brenner 1979), but they are infrequent, and clear evidence of typical storm-generated features such as hummocky cross-stratification is lacking, suggesting deposition on a low-energy coast (Clifton 2006). Facies S1 contains up to two regionally traceable horizons of calcite-cemented concretions, the lower of which is abundantly fossiliferous, including the ammonite *Cardioceras*. These concretions are similar to those reported to the east from Natrona and Carbon counties by Andersson (1979).

Facies S2 gradationally overlies Facies S1 and records deposition in a shoreface setting. The presence of pervasive wave-ripple and current-ripple lamination (Fig. 5B) rather than hummocky cross-stratification and trough cross-bedding supports the interpretation of a low-energy setting (Raaf and van Gelder 1977; Clifton 2006). The trace fossil association indicates a *Skolithos* ichnofacies, additional evidence of a shallow-water setting.

Facies S3 also gradationally overlies Facies S1 and is interpreted as recording upward shallowing and the formation of a shell bed (Kidwell 1991). Two such shell beds are present (Fig. 5C, D), and they are regionally traceable (Fig. 6). The lower shell bed is overwhelmingly

TABLE 2.—*Wave-dominated Siliciclastic Shelf Facies Association S.*

Facies	Sedimentology	Paleontology	Geometry and contact relationships
S1—offshore	Olive gray glauconitic and bioturbated mudstone to siltstone grading upwards into tan sandy mudstone and sandy siltstone. Bivalve fragments present locally and commonly neomorphosed. Shell beds 2–20 cm thick locally developed and dominantly composed of bivalves. Up to two horizons of light gray or rusty carbonate concretions, with lower horizon containing common trace and body fossils.	Belemnites (*Pachyteuthis*) typically highly abundant. Gastropods and ammonites (*Cardioceras*) locally common, usually in concretions with other bivalves (*Astarte*, *Pleuromya*, *Vaugonia*). Rare echinoids. Ostracods. Articulated skeletons and isolated bones of plesiosaurs (*Pantosaurus*, *Tatenectes*) and ichthyosaurs (*Ophthalmosaurus*). Trace fossils include *Planolites* and *Rhizocorallium*, mostly preserved within concretions.	Tabular units up to 65 m thick. Gradationally overlain by Facies S2, and sharply overlain by several facies of estuarine association T.
S2—shoreface	Tan, fine-grained to very fine-grained, sublitharenite to quartz arenite, often argillaceous and interbedded with silty mudstone to siltstone. Sandstone beds 2–10 cm thick, increasing in number and thickness upsection, and containing common wave-ripple lamination, planar lamination, and current-ripple lamination. Glauconite is common as peloids, as are grains of black chert. Sand cemented with carbonate, with minor pyrite and goethite.	Rare poorly preserved internal molds of bivalves. Rare bone, including the plesiosaur *Tatenectes*. Trace fossils common, including *Planolites*, *Chondrites*, *Skolithos*, and *Schaubcylindrichnus*.	Tabular units up to 10 m, generally thinner, and usually truncated by an erosional surface overlain by facies of the estuarine association T.
S3—shell beds	Highly shelly very fine-grained sublitharenite to quartz arenite in beds 2–30 cm thick, separated by thin mudstone partings and lacking sedimentary structures. Glauconite is common as peloids. Shells are densely packed in beds that thicken upwards. Preservation of shells varies widely, from nearly pristine articulated shells, to isolated valves, to highly fragmented shells ranging down to sand-sized grains. Individual beds have crude normal grading, but lack other sedimentary structures.	Bivalves (*Liostrea* or *Camptonectes*) abundant, often in nearly monospecific accumulations. Rare to uncommon crinoid columnals (*Isocrinus*)	Tabular units, generally less than 1 m thick. Gradational contact with underlying facies S1, but sharp contact with overlying facies S1.

composed of the oyster *Liostrea*, and the upper shell bed is dominated by the scallop *Camptonectes*. Similar *Camptonectes* beds occur in upper Oxfordian deposits of Milne Land, East Greenland and have been interpreted as offshore storm events that reworked accumulations of *Camptonectes* shells (Fürsich and Heinberge 1983). Individual beds within Facies S3 also likely have a storm origin (Specht and Brenner 1979).

Overall, the wave-dominated shelf facies association reflects deposition on a relatively protected, low-energy siliciclastic margin. Low-energy wave-dominated coasts differ from high-energy coasts in that low-energy systems generally have thinner deposits, their maximum grain size is typically fine grained, and their deposits lack upper flow regime sedimentary structures (Clifton 2006). Modern low-energy analogs are present in southeastern Spain and along the southeastern U.S. coast (Howard et al. 1972; Clifton 2006). Studies from the mesotidal coast of the southeastern United States indicate that the largest grain size seen in low-energy coasts is typically fine-grained sand because wave-generated flows are too weak to transport coarser sediment (Howard et al. 1972). No foreshore sediments were recognized in the Sundance Formation, reflecting relatively weak waves, but possibly also because they were eroded during the formation of the overlying sequence boundary.

Tidal Estuary Facies Association T

The tidal estuary facies association consists of four facies interpreted to have been deposited in tidal channel (T1), tidal bar (T2 and T3), and tidal sand flat (T4) environments (Table 3). The tidal estuary facies association is present in two intervals of the Sundance Formation. The first comprises the upper Hulett Member (of DeJarnette and Utgaard 1986) in the middle of the Sundance Formation, and the second comprises the entire Windy Hill Sandstone that caps the Sundance Formation (Uhlir et al. 1988).

Facies T1 represents channel-bottom deposits, based on the abundance of shells, mudstone intraclasts, chert pebbles, and the coarsest grain size of sand present in the Sundance Formation (Fig. 7A, B; Uhlir et al. 1988). Lateral accretion surfaces reflect the migration of adjacent bars, and trough cross-stratification indicates the presence of dunes. Bivalves, rare echinoderms, and rare belemnites indicate a marine influence. The local dominance of *Liostrea* suggests brackish conditions, whereas the local dominance of *Ceratomya* indicates areas of near-normal marine salinity (Fürsich et al. 1995). Facies T1 typically overlies a highly erosional surface at the base of the Windy Hill Sandstone (discussed below), but can also occur repeatedly within individual outcrops of the Windy Hill.

Facies T2 and T3 represent tidal bars, based on their typical occurrence above Facies T1 and abundant tidal features including tidal bundling, clay drapes, reactivation surfaces, and reversing paleocurrent directions (Fig. 7C; Uhlir et al. 1988). Facies T2 is characterized by trough cross-stratification, indicating dunes, which is variably bioturbated with a *Skolithos* ichnofacies. Planar lamination within Facies T2 may record episodically elevated shear stress, or it may indicate foreshore settings within the outer portions of the estuary (Uhlir et al. 1988). Facies T3 has distinctive sigmoidal cross-stratification (Fig. 7D), formed by neap-spring tidal variations and common in the open, sandy portions of estuaries (Kreisa and Moiola 1986; Shanley et al. 1992).

Facies T4 records deposition on tidal sand flats, based on its typical association overlying Facies T2 and T3, its finer grain size than the other facies tidal estuary association, and the abundance of wave-ripple and current-ripple lamination (Fig. 7E). Common climbing ripples record local rapid deposition at the edges of the sand flats. Both inside and

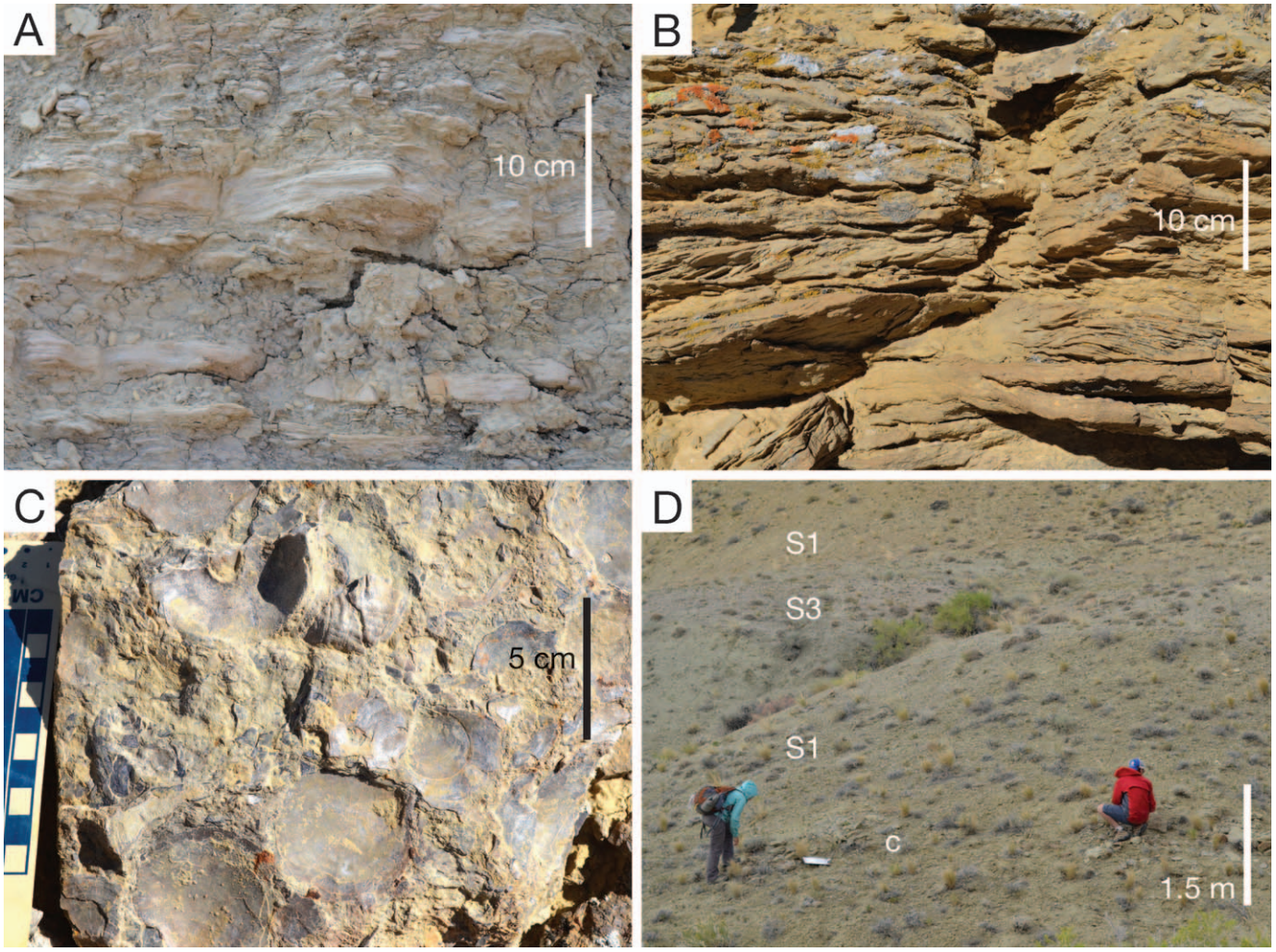

FIG. 5.—Wave-dominated siliciclastic shelf facies association. **A**) Facies S1 (offshore), with a few very thin beds of rippled sand. **B**) Facies S2 (shoreface), displaying rippled very fine sandstone. **C**) Bedding-plane view of Facies S3 with abundant valves of the scallop *Camptonectes*. **D**) Facies S3, encased in Facies S1, illustrating minimal differences in weathering of these facies. c = horizon of fossiliferous concretions.

outside of the Bighorn Basin, rippled sand facies within the Windy Hill preserve pterosaur tracks (e.g., Logue 1977; Lockley and Wright 2003; Harris and Lacovara 2004; Connely 2006).

Elements of the tidal estuary facies association are typically arrayed in fining-upward successions, with Facies T1 (tidal channel) at the base, overlain by Facies T2 and T3 (tidal bar), and capped by Facies T4 (tidal sand flat). Most successions preserve only a portion of this sequence, owing to channel migration. Paleocurrent measurements on large-scale foresets within this facies association indicate northwest-southeast bimodal tidal flow within sandstone facies (T2 and T3), and east-west lateral channel migration within the coquina channel lag (T1) facies (Uhlir et al. 1988).

SUNDANCE SEQUENCE STRATIGRAPHY

The Sundance Formation contains four depositional sequences (Figs. 6, 8A). The first two sequences are built from the carbonate ramp facies association. The third sequence is primarily composed of the tidal estuary and wave-dominated shelf facies associations, and the fourth is entirely tidal estuary facies association. The sequence-bounding unconformities correspond to previously recognized regional unconformities (Pipiringos 1968; Pipiringos and O'Sullivan 1978).

Sequence J2

Sequence J2 is represented by Canyon Springs Member and Stockade Beaver Shale. The basal sequence boundary is marked by a sharp contact with structureless red mudstone of the Gypsum Spring and Piper formations. The contact is locally mantled by chert pebbles (Pipiringos 1968). At Ten Sleep, for example, the contact is overlain by a 30 cm conglomerate of well-rounded, poorly sorted chert pebbles, typically with diameters of 1–2 cm, but up to 10–13 cm. In most places, chert pebbles are scarce.

The lower part of the J2 sequence consists of 2–3 carbonate parasequences. To the north, these are composed of facies deposited in a shallow subtidal environment (C2). Southward, these parasequences have thicker caps of bioturbated skeletal to oolitic wackestone and packstone, which pass into oolitic facies (C3) farther to the south. This regional transition suggests that the southern end of the transect is a relatively shallower water setting than the northern end. The tops of these parasequences are commonly wave rippled. Some comprise firmgrounds or hardgrounds, with microbial mats, casts of salt crystals, *Diplocraterion* and *Rhizocorallium*. At least one of these parasequence tops bears abundant tridactyl dinosaur tracks attributed to a small theropod (Kvale et al. 2001,

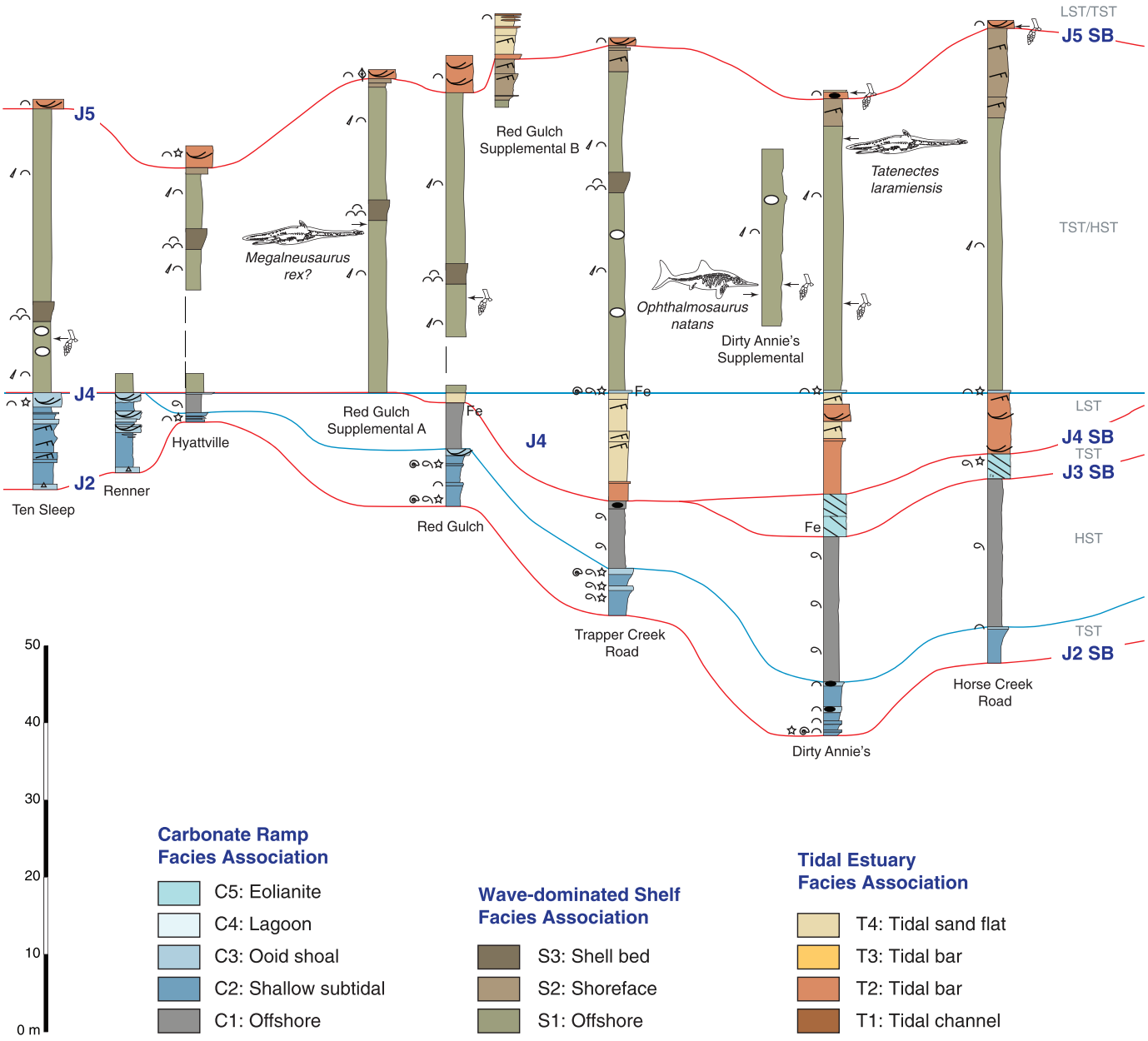

FIG. 6.—Stratigraphic cross section of the Sundance Formation on the east flank of the Bighorn Basin, Wyoming.

2004; Mickelson et al. 2006; Clark and Brett-Surman 2008). Stacking patterns in these parasequences appear to be aggradational: they all contain the same facies, with no obvious regionally consistent upward trend in facies composition or thickness. These carbonate strata are sharply overlain by mudstone facies (C1) of the Stockade Beaver Shale, which contains extraordinarily abundant, largely disarticulated valves of *Gryphaea nebrascensis*. With the aggradational stacking of shallow-water carbonates, the Canyon Springs is interpreted as the transgressive systems tract (TST), with a major flooding surface at its upper contact with the Stockade Beaver Shale. The Stockade Beaver Shale may represent parts of the transgressive and highstand systems tracts (HST), but it lacks any evidence of facies variation or an obvious maximum flooding surface or zone.

Sequence J3

Sequence J3 is represented by a portion of the Hulett Member, specifically the lower and middle carbonate members of DeJarnette and Utgaard (1986). The basal sequence boundary is marked by a sharp

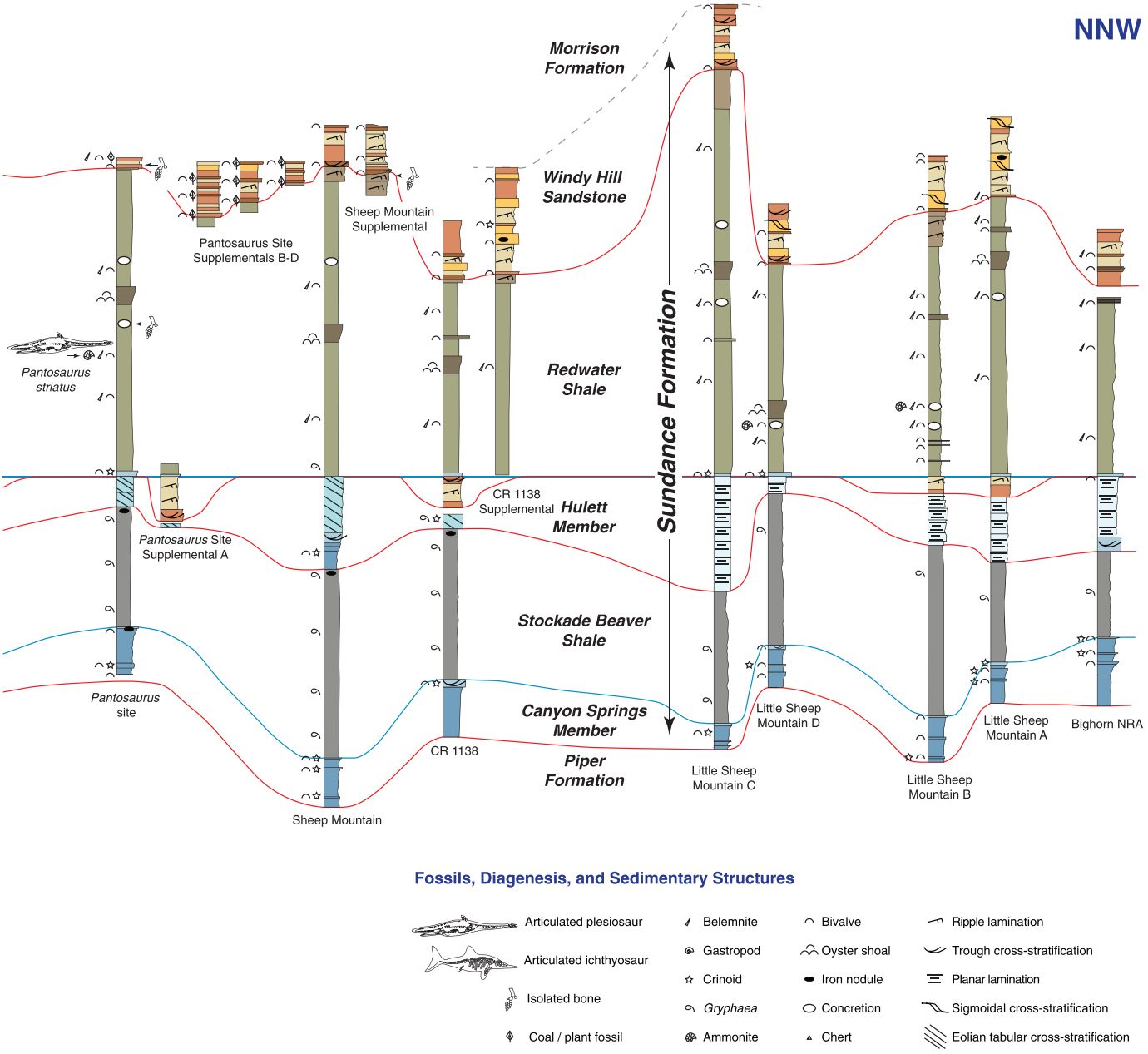

FIG. 6.—Continued.

contact of shallow-water carbonate facies on the offshore mudstone of the Stockade Beaver Shale (Fig. 8B). To the north, these are facies deposited primarily in lagoonal (C4) and sometimes ooid shoal (C3) environments. Facies deposited in an eolian setting (C5) typically lie above this contact in the central portion of the transect, although locally facies deposited in a shallow subtidal environment (C2) do. The uppermost mudstone of the Stockade Beaver Shale is commonly stained red beneath this unconformity. The base of the Hulett Member was thought by Pipiringos and O'Sullivan (1978) to be the J3 unconformity in the Bighorn Basin. The J3 unconformity is truncated by the J4 unconformity in the southernmost part of the study area, suggesting uplift on the Sheridan Arch (Pipiringos and O'Sullivan 1978; Schmude 2000).

Little of the J3 sequence is preserved, and most exposures display only a single facies, making assignment to any systems tract uncertain. At Sheep Mountain (Fig. 6), basal facies of the Hulett deposited in a shallow subtidal environment (C2) are gradationally overlain by facies deposited in an ooid shoal environment (C3), capped by facies deposited in an eolian environment (C5). Whether this represents a single parasequence or progradational stacking is unclear. Depositionally downdip, at Bighorn NRA (Fig. 6), basal ooid facies (C5) are overlain by facies deposited in a lagoonal setting (C4), also suggesting upward shallowing.

Sequence J4

Sequence J4 consists of the upper Hulett Member (of DeJarnette and Utgaard 1986) and the Redwater Shale. Stratigraphic relationships within the J4 sequence are often difficult to recognize in the field, owing to

TABLE 3.—*Tidal Estuary Facies Association T.*

Facies	Sedimentology	Paleontology	Geometry and contact relationships
T1—tidal channel	Medium-grained sublitharenite to litharenite with abundant and typically densely packed broken (~ 1 cm across) and abraded bivalves, with less common wood and bone. Grains of glauconite and black chert are common. Coarse calcite cement. Hematite-cemented sandstone rip-up clasts and mudstone rip-up clasts (to 3 cm) locally present. Trough cross bedding common (20–50 cm sets), and tabular cross beds up to 1.5 thick locally developed, as are sets of lateral accretion surfaces.	Abundant bivalves, primarily *Liostrea* and *Ceratomya*, but also *Tancredia*, *Camptonectes*, *Quenstedtia*. Crinoid columnals and belemnites locally present. No trace fossils observed.	Lens-shaped with highly erosional base, with up to 10 m of relief visible at a single outcrop. Overlain by facies of the estuarine association (most often T2 or T3), or in some cases, presumed Morrison Formation, although such contacts are usually poorly exposed on steep dip slopes.
T2—tidal bar	Very fine-grained to medium-grained sublitharenite, generally with trough cross-bedding in 20–60 cm sets, but locally highly bioturbated. Beds of planar lamination are also present. Calcite-cemented, with sparse micritized skeletal grains. Mudstone rip-up clasts locally present. Clay drapes on foresets are common, as are reactivation surfaces, herringbone cross-stratification, and tidal bundling of foresets.	Rare to locally common bivalves, typically small *Liostrea*. Trace fossils include *Diplocraterion*, *Skolithos*, and *Schaubcylindrichnus*.	Lens-shaped bodies up to several meters thick. Commonly overlies Facies T1 and overlain by Facies T4, but can have sharp contacts with any facies of the estuarine association T.
T3—tidal bar	Similar to Facies T2, but with distinctive tidally bundled sigmoidal cross-bedding in sets 40–80 cm thick. Calcite cemented.	Lacks body and trace fossils.	Lens-shaped bodies up to a few meters thick. Generally associated with Facies T2 and overlain by facies T4.
T4—tidal sand flat	Very fine-grained to fine-grained sublitharenite in beds 2–25 cm thick. Pervasively ripple-laminated, primarily current-generated, but also some wave-generated forms. Climbing ripple lamination is common. Locally with 0.5–2 cm argillaceous interbeds and 15–20 cm beds of shelly rippled sand. Rare coal laminae. Calcite cemented.	Rare bivalves, primarily in thin shell beds.	Lens-shaped bodies up to 7 m thick. Commonly overlies Facies T2 and T3, but sharply overlain by other facies of the estuarine association.

widespread slumping and deep weathering. Because the thickness of the Redwater Shale is relatively uniform in well-log data (Fig. 9), pronounced variations in outcrop thicknesses of the Redwater Shale over relatively short distances (e.g., Little Sheep Mountain C and D, Fig. 6) are attributed to slumping and duplicated sections. Likewise, shelly horizons within the Redwater Shale have consistent positions in well logs (Fig. 9), and their stronger variation in position within outcrops (Fig. 6) is also attributed to slumping.

The basal sequence boundary of the J4 sequence is an erosional surface, with up to 10 m of relief visible at a single outcrop (Fig. 8B), with erosional lows filled with sandstone of the upper Hulett (of DeJarnette and Utgaard 1986). This erosional surface also displays regional truncation, progressively removing the lower and middle Hulett carbonates to the south, followed by the Stockade Beaver Shale, and the upper portion of the Canyon Springs Member (Fig. 6). Where the Stockade Beaver Shale underlies the J4 unconformity, the upper meter is stained red (e.g., Red Gulch, Fig. 6). Where the Hulett eolianites underlie this surface, the upper half-meter is chalky. In some places, no incision is present, and the Redwater Shale rests directly on the lower or middle Hulett carbonates (e.g., Bighorn NRA, Sheep Mountain, Fig. 6). The upper Hulett, which fills erosional lows along this sequence boundary, consists of facies deposited in tidal bar (T2) and tidal sand flat (T4) environments, and it is interpreted as the lowstand systems tract (LST), although it may represent initial TST deposits. Chert pebbles are known from the base of the Redwater Shale and have been used to infer the presence of the J4 unconformity (Pipiringos 1968; Pipiringos and O'Sullivan 1978). We suggest that the J4 unconformity lies at the base of the Redwater Shale where the upper Hulett is absent, and that it lies underneath the upper Hulett where it is present.

Throughout the region, the Hulett is sharply overlain by offshore mudstone (S1) of the belemnite-rich Redwater Shale, marking a prominent and major flooding surface. At some localities, the base of the Redwater has a 50 cm glauconitic and sandy cross-bedded oolitic to shelly grainstone. In other localities, the base of the Redwater is marked by up to 30 cm of current-ripped to wave-rippled pyritic quartz arenite, which in a few cases overlies the oolitic to shelly grainstone. Wave-ripple crests on this bed are oriented ENE-WSW, consistent with a roughly east-west oriented shoreline. In other places, the base of the Redwater has a 3–15-cm-thick megarippled shell bed. The transgressive surface is placed underneath these distinctive beds, which are interpreted to reflect various forms of stratigraphic condensation during flooding into offshore settings.

The Redwater Shale contains several weakly developed parasequences, defined primarily by evidence of stratigraphic condensation rather than facies changes. The first of these flooding surfaces is placed at a horizon of rusty carbonate concretions up to half a meter across (Fig. 5D). These concretions preserve *Rhizocorallium* and *Thalassinoides* traces, suggesting firmground conditions. These concretions can be richly fossiliferous with abundant bivalves, and rare crinoids, belemnites, and ammonoids, some with preserved color patterns. Some of the concretions preserve ichthyosaur bone and decapods (Wahl 2008).

The second and third flooding surfaces are marked by shell beds (Facies S3; Figs. 5D, 8A), the first having abundant oysters (*Liostrea strigilecula*), and the second having abundant scallops (*Camptonectes bellistriatus*). A second horizon of concretions—white and sparsely fossiliferous—occurs above the scallop shell bed. These surfaces are regionally traceable on spontaneous potential well logs (Fig. 9), and their well log signatures may reflect variations in cementation. Well-log expression suggests that the lowest of these flooding surfaces (the rusty,

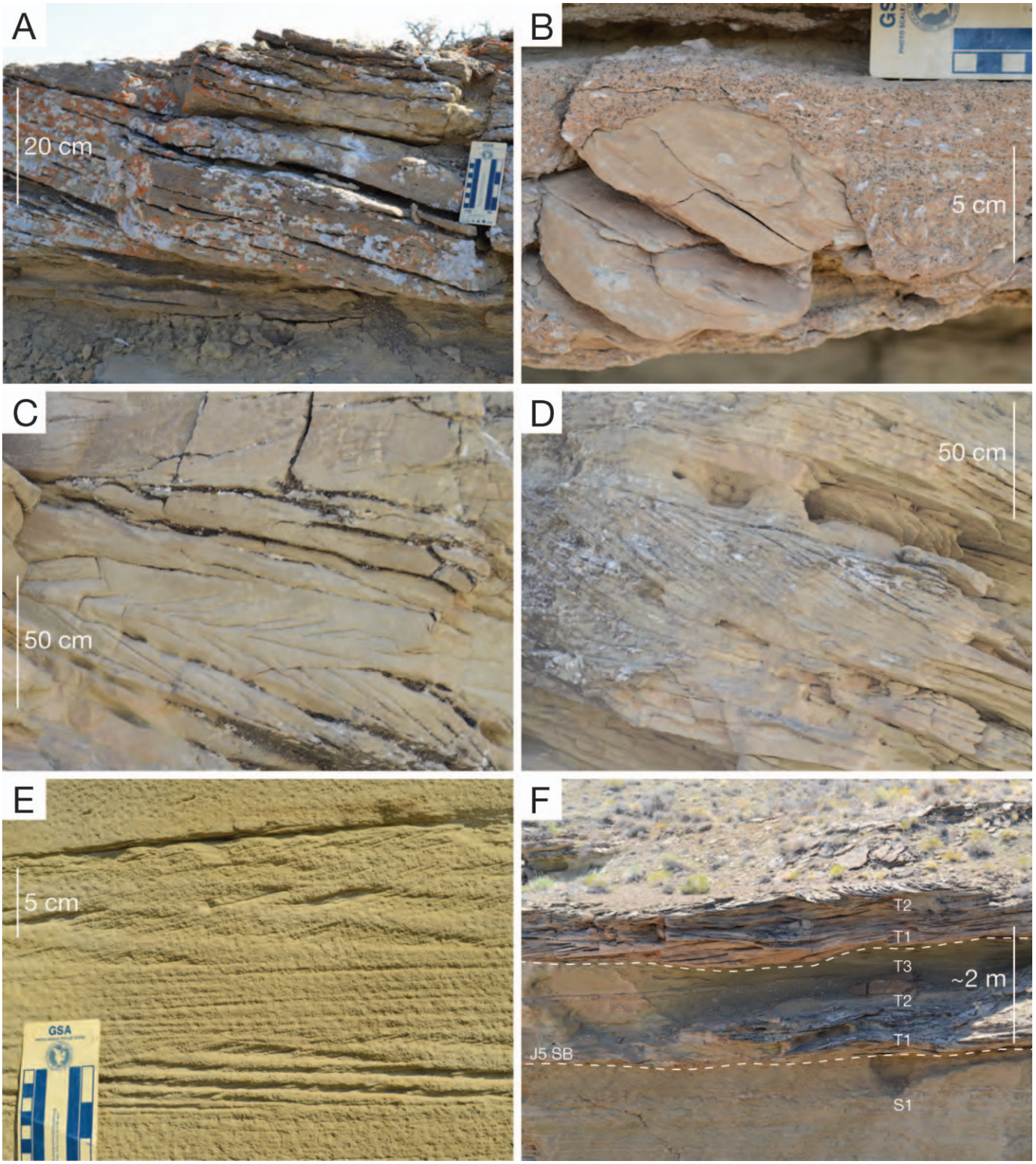

FIG. 7.—Tidal estuary facies association. **A**) Facies T1 (tidal channel), showing large scale foresets developed in coarse shelly sand. **B**) Facies T1, with large sandstone rip-up clast in a matrix of coarse sand and shells. **C**) Facies T2 (tidal bar), with opposing paleocurrent directions. **D**) Facies T3 (tidal bar), with sigmoidal cross-bedding. **E**) Facies T4 (tidal sand flat), with climbing ripples of very fine sand. **F**) Upward-fining cycles composed of Facies T1 (tidal channel), T2 (tidal bar), and T3 (tidal sand flat). Basal erosional surfaces indicated with dashed lines; lower surface is the J5 sequence boundary. S1 = Redwater Shale.

FIG. 8.—Sequence stratigraphic architecture. **A**) Overview of the Sundance Formation at Camp Skeeter. CS = Canyon Springs Member; SBS = Stockade Beaver Shale; H = Hulett Member; RS = Redwater Shale; WH = Windy Hill. Dashed lines: tops of shell-bed–capped parasequences. J3–J5 sequence boundaries indicated. **B**) Incised valley fill at J4 unconformity at *Pantosaurus* locality. Abbreviations as in part A, with Hl = lower Hulett, and Hu = upper Hulett. Long-dashed line is J3 sequence boundary, solid line is J4 sequence boundary displaying truncation of underlying sequence, and short-dashed line is major flooding surface at the base of the Redwater Shale. **C**) J5 sequence boundary (solid line) east of the Red Gulch Dinosaur Trackway, showing truncation of underlying shoreface-capped parasequences of the Redwater Shale, with flooding surfaces indicated by dashed lines. S = slumped block. Abbreviations as in part A.

fossiliferous concretions) is the most distal, making it the maximum flooding surface. The Redwater Shale beneath this concretion horizon locally contains thin sandy and shelly storm beds (Brenner and Davies 1973), which are largely absent above the concretions, consistent with the concretion horizon marking the maximum flooding surface. In the uppermost Redwater, facies deposited in an offshore environment (S1) pass upward into facies deposited in the shoreface (S2), consistent with overall progradational stacking in the HST.

Sequence J5

Sequence J5 consists of the Windy Hill Sandstone and likely some portion of the overlying Morrison Formation. The J5 sequence boundary is a highly erosional surface (Fig. 8C) and has been recognized previously as a regional unconformity (Pipiringos 1968; Pipiringos and O'Sullivan 1978; Ahlbrandt and Fox 1997). It commonly displays meters, and in some cases, more than 10 meters of relief within a single outcrop. Where the depth of erosion is great, facies deposited in the shoreface (S2) are missing from the top of the Redwater, and the Windy Hill rests directly on the mudstone (S1) of the Redwater.

The tidal estuary deposits of the Windy Hill Sandstone overlie the J5 sequence boundary throughout the study area. The thickness of the Windy Hill directly reflects the depth of erosion, and this thickness varies markedly over short distances. These thickness variations affect the development of the erosional hogback supported by the Windy Hill. The hogback is prominent where the J5 unconformity is deeply incised and it is minor to absent where little erosion has occurred on the J5 unconformity.

In most places, the basal beds of the Windy Hill are composed of shelly and coarse-grained facies interpreted as tidal channel (T1). These basal beds often contain rip-up clasts of mudstone and cemented sandstone of the Redwater Shale (Fig. 7B), as well as chert pebbles, wood, and bone fragments. In some places, distinct fining-upward cycles that record deposition in tidal channel (T1), tidal bar (T2 and T3), and tidal sand flat (T3) environments are developed (Fig. 7F). In most places, transitions between these facies are abrupt and unpredictable. Furthermore, individual facies bodies often cannot be traced laterally for more than a few tens to hundreds of meters. The shelly beds have been previously interpreted as shell sand ridges (Brenner et al. 1985), but this is inconsistent with the deeply incised basal surface, and presence of facies typical of tidally influenced estuarine systems.

The contact with the overlying Morrison was not observed in the study area, as it is generally covered on the dip slope formed by the Windy Hill hogback. Where others have seen the transition, both within and beyond the Bighorn Basin (e.g., Johnson 1992; Peterson 1994), they have described it as gradational, suggesting that the tidal estuarine facies association of the Windy Hill may pass upward into a tidal delta facies association, followed by coastal plain deposits of the Morrison. Because the estuarine deposits of the Windy Hill were never overstepped by marine facies, it is not possible to identify a transgressive surface, and the systems tract that the Windy Hill represents is uncertain.

SUNDANCE FOSSIL DISTRIBUTION

Invertebrate Fossils

The occurrence of invertebrate fossils is strongly controlled by overall stratigraphic position and depositional environment, and this is best

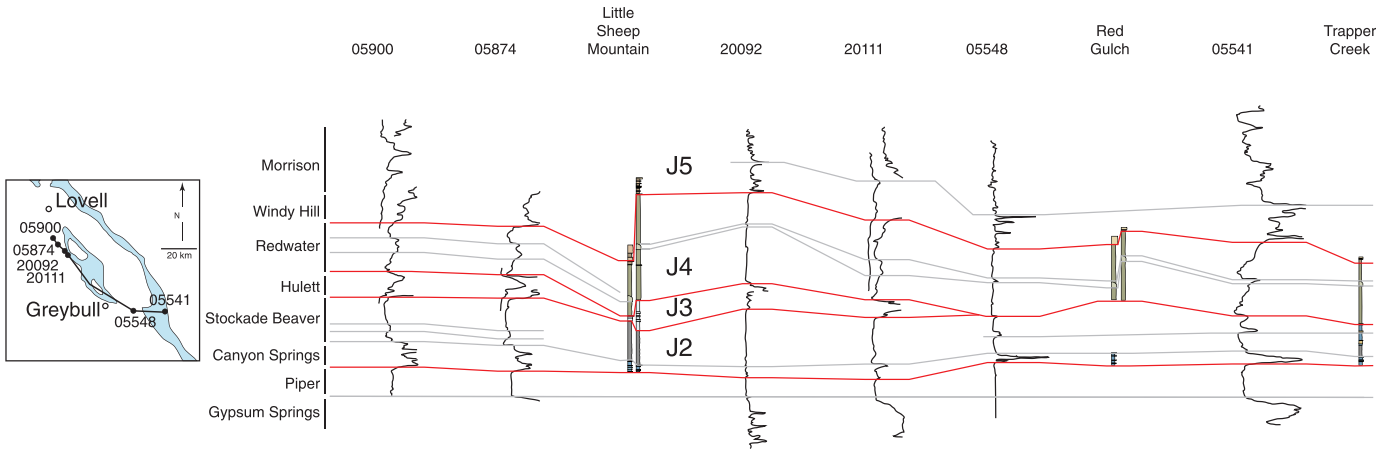

FIG. 9.—Correlation of spontaneous potential well logs and selected outcrops along the east flank of the Bighorn Basin, Wyoming. Comparison of well logs to nearby outcrops indicates that positive (rightward) excursions on the logs correspond to porous units such as sands and shell beds, whereas negative (leftward) excursions correspond to intervals of mudstone. Red lines indicate sequence-bounding unconformities. Gray lines indicate flooding surfaces and, within the J4 sequence, the upper and lower contacts of shell beds. Resistivity logs in this area generally show little variation through the Sundance Formation and are not displayed.

shown by nonmetric multidimensional scaling (NMS ordination) of field censuses (Fig. 10).

Samples from the upper and lower Sundance cleanly separate, primarily along NMS axis 1, with lower Sundance samples having typically larger scores than upper Sundance samples (Fig. 10A). Lower Sundance samples are usually dominated by some combination of the oyster *Gryphaea nebrascensis*, the crinoid *Chariocrinus*, and indeterminate bivalves and gastropods, whereas upper Sundance samples contain the oyster *Liostrea strigilecula*, belemnites, the crinoid *Isocrinus*, the ammonoid *Cardioceras*, and an array of bivalves, including *Astarte*, *Vaugonia*, *Tancredia*, and *Myopholas* (Fig. 10B). The faunal distinctiveness of the lower and upper Sundance likely reflects the overall depositional setting of the two units, with the lower Sundance being carbonate dominated and the upper Sundance being siliciclastic dominated. The faunal distinctiveness may also reflect a substantial difference in age between the lower and upper Sundance. Except where the upper Hulett incised valley fill is present, the boundary between the lower and upper Sundance corresponds the J3 unconformity. This unconformity is thought to represent the longest hiatus within the Sundance (Imlay 1980), spanning the middle and upper Callovian, and representing up to 2 myr.

Faunal assemblages from the lower Sundance differ among lithofacies. Canyon Springs facies that record shallow subtidal deposition (C2) commonly contain abundant bivalves, common crinoid columnals (*Chariocrinus*), and rare gastropods. Bivalves are typically preserved as molds, making identification difficult, with the exception of *Myopholas*. The available ooid shoal samples tend to lack *Myopholas* and gastropods, but they contain common fragmentary bivalve molds that are rarely identifiable. The Stockade Beaver Shale is distinct from both facies of the Canyon Springs because it contains a virtually monospecific fauna of extraordinarily abundant *Gryphaea nebrascensis* (Fig. 11A). Such samples are not shown on the ordination because monospecific samples tend to distort relationships among samples in ordinations and are culled before analysis.

Within the upper Sundance, samples also segregate by lithofacies (Fig. 10C), with some overlap. Mudstone (S1) of the Redwater Shale is generally dominated by nearly monospecific accumulations of the belemnite *Pachyteuthis densus*. More rarely, these are associated with sparse small shells of *Liostrea strigilecula* and *Camptonectes bellistriatus*.

Near flooding surfaces, three distinct associations form within the offshore of the Redwater Shale. The lowermost of these associations is present at the lower concretion horizon in the northern part of the field area (e.g., Little Sheep Mountain). These concretions contain a diverse assemblage of bivalves (*Astarte*, *Liostrea*, *Pleuromya*, *Vaugonia*), belemnites (*Pachyteuthis*), ammonoids (*Cardioceras*), and crinoids (*Isocrinus*). Preservation is generally good with minimal breakage and abrasion, with common articulation of bivalves. The second association occurs at a shelly horizon at the top of a parasequence. This interval is dominated almost exclusively by the oyster *Liostrea strigilecula*. These shells are nearly always disarticulated, with moderate amounts of breakage and abrasion. The abundance of shells varies laterally in an outcrop, giving the appearance of isolated shoals, but areas between these concentrations also contain shells and well-log tracing indicates that this horizon is regionally persistent. The third association occurs in a shell bed at a parasequence near the top of the Redwater Shale, and it contains dense accumulations of the scallop *Camptonectes bellistriatus* (Fig. 5C). These show a wide range of preservation, including beds of articulated and whole valves to beds of highly fragmented shells.

Finally, tidal estuarine deposits in the Windy Hill Sandstone have localized, monospecific accumulations of *Ceratomya* (Fig. 11B), as well as accumulations dominated by *Liostrea strigilecula*, with the bivalves *Tancredia*, *Camptonectes*, and *Quenstedtia*. Most shells are disarticulated, fragmented, and abraded, suggesting substantial local reworking. In addition are rare specimens of belemnites and crinoids that are so highly abraded and fragmented that they are likely reworked from the underlying Redwater Shale.

Vertebrate Fossils

Marine reptiles are found in the Redwater Shale and Windy Hill Sandstone, where they occur along flooding surfaces, along sequence boundaries, and within facies recording offshore (S1) and shoreface (S2) deposition.

Vertebrate fossils are found along the maximum flooding surface in the Redwater Shale in the northern part of the study area. These fossils are often preserved in fine-grained concretions, with good surface detail, both as isolated bones and partially disarticulated but associated remains (Fig. 10B, C). The assemblage is limited, and consists of one ichthyosaur species (*Ophthalmosaurus natans*) and one plesiosaur species (*Pantosaurus striatus*; Wahl et al. 2007). Remarkably, one of these plesiosaur specimens recently discovered at the *Pantosaurus* site (Fig. 6) has an ichthyosaur embryo in its stomach contents (O'Keefe et al. 2009).

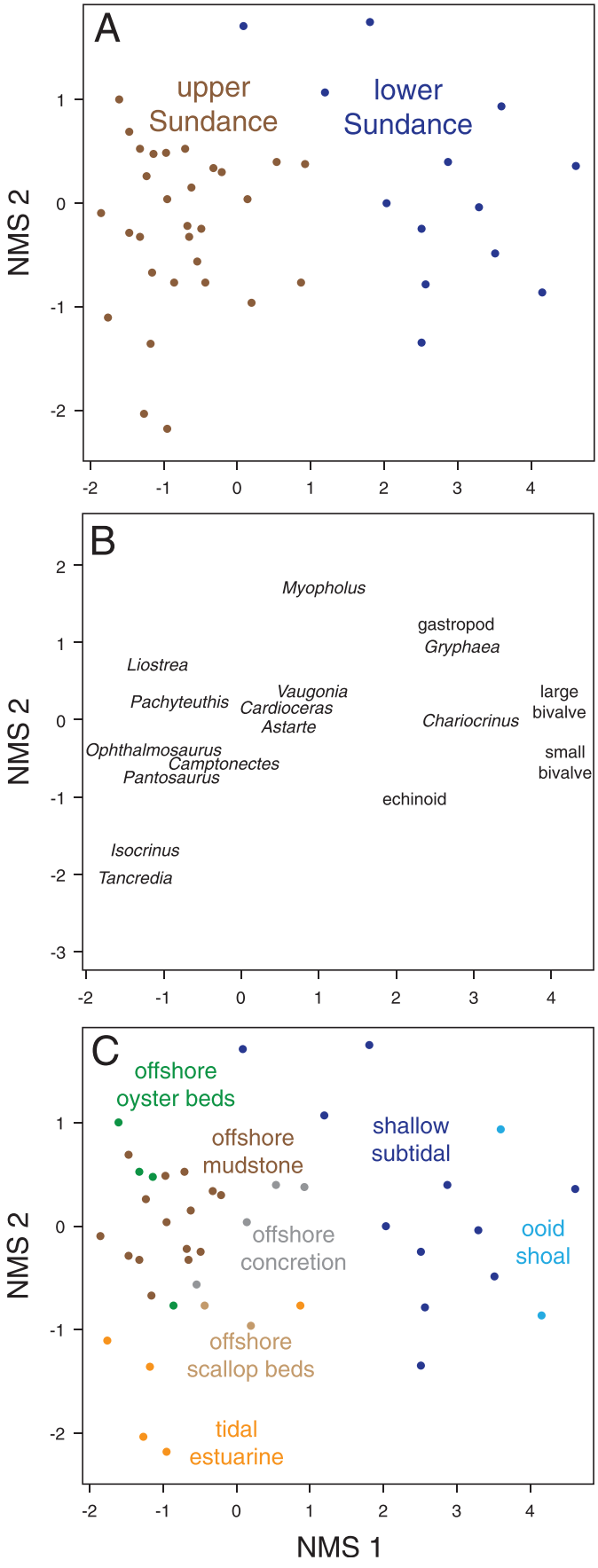

Vertebrate fossils are also found in association with J5 sequence boundary, where isolated highly abraded bone fragments are found in tidal channel deposits (T1) that immediately overlie the sequence boundary. The preservation of these fragments is so poor that neither the taxon nor the element can generally be determined. Given its state of preservation, some or all of this material may represent material reworked from the erosion of the underlying Redwater Shale.

Some vertebrate fossils are found in facies recording offshore (S1) and shoreface (S2) deposition in the Redwater Shale, but not associated with any significant stratigraphic surface (Fig. 11C). The offshore mudstone locally bears bone directly below the oyster shell beds (S3). Although this material is most commonly disarticulated and somewhat abraded, articulated specimens have been found, including the ichthyosaur *Ophthalmosaurus natans*, the plesiosaur *Pantosaurus striatus*, and the pliosaur, *Megalneusaurus rex*. Facies S2 contains rare disarticulated to partially articulated vertebrate fossils, including a partial skeleton of the plesiosaur *Tatenectes laramiensis* near the Dirty Annie's locality (Fig. 6, O'Keefe and Street 2009). Elements of this skeleton were closely associated, but not articulated (O'Keefe and Street 2009). More articulated specimens are needed to know if the associations of these species with the offshore and shoreface reflect where these species lived or whether carcasses underwent substantial postmortem transportation.

DISCUSSION

Occurrence of Invertebrate Fossils

Numerous field and modeling studies have demonstrated the multiple ways in which the stratigraphic distribution of marine fossils is controlled by sequence architecture (summarized in Patzkowsky and Holland 2012). Patterns of invertebrate occurrence in the Sundance agree well with these studies.

Invertebrate fossils in the Sundance are strongly tied to lithofacies. For example, the offshore mudstone (C1) of the Stockade Beaver Shale is diagnostically recognized by an extraordinary profusion of the oyster *Gryphaea nebrascensis*, and the offshore mudstone (S1) of the Redwater Shale is likewise dominated by the belemnoid *Pachyteuthis densus*. The density of these is staggering: assuming a conservative density of 100 individuals per square meter, there are over one quadrillion belemnoids preserved just in the Bighorn Basin portion of the Sundance Sea, and a similar number of oysters. Even so, *Gryphaea nebrascensis* is uncommon in facies deposited in shallow subtidal (C2), ooid shoal (C3), and lagoon (C4) environments in the Canyon Springs and Hulett Members, and belemnoids are scarce to absent in facies deposited in the shoreface (S2) of the Redwater Shale. Although such variations in abundance are likely obvious even to casual observers, other shifts in relative abundance among facies are subtler. Ordination of field-based relative abundance indicates that ooid shoal and shallow subtidal carbonates differ, and that offshore mudstone, offshore concretions, offshore oyster beds, offshore scallop beds, and tidal estuarine siliciclastic facies also differ from one another (Fig. 10).

Concentrations of invertebrate fossils show a strong and expected correspondence with zones of low net sedimentation (Kidwell 1991). This correspondence is best seen in the siliciclastic upper Sundance Formation, where concentrations of invertebrates are present in two contexts.

←

FIG. 10.—Nonmetric multidimensional scaling of fossil assemblages in the Sundance Formation. **A**) Sample scores coded by the carbonate-dominated lower Sundance and the siliciclastic-dominated upper Sundance. **B**) Taxon scores. **C**) Sample scores coded by lithofacies.

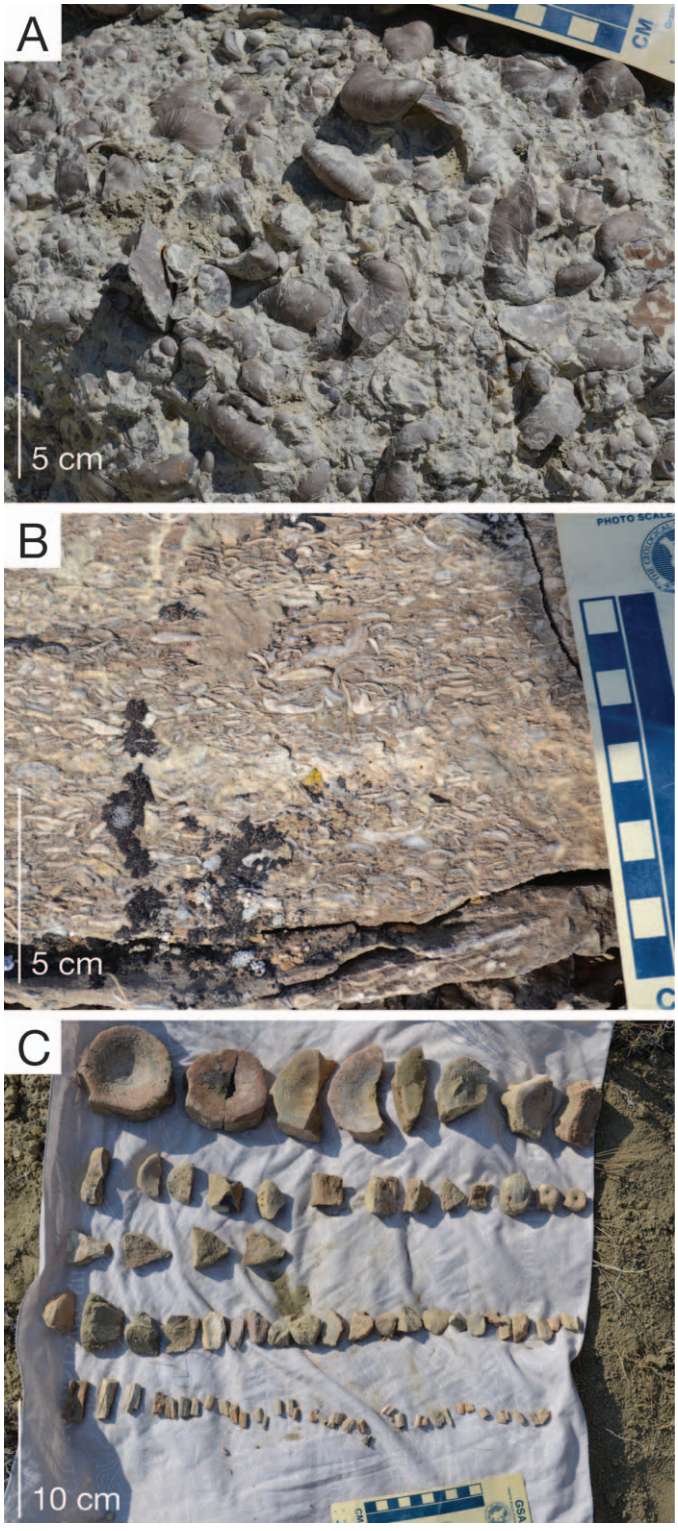

FIG. 11.—Fossil concentrations. **A**) Densely packed shells of *Gryphaea nebrascensis*. **B**) Densely packed shells of *Ceratomya*. **C**) Ichthyosaur vertebrae and rib fragments.

The first of these contexts is the diverse association of well-preserved invertebrates in concretions in the lower part of the Redwater Shale. Based on stacking patterns best expressed in well logs (Fig. 9), these concretions are interpreted to have formed at the maximum flooding surface of the J4 sequence. This fossil association is the most diverse one in the Redwater Shale, and it is the only horizon characterized by common ammonites, primarily *Cardioceras*. Not all concretions within the Redwater Shale are fossiliferous. A second concretionary horizon near the top of the Redwater Shale only rarely contains fossils. The concentration of fossils and the presence of concretions are both suggestive of a condensed section, formed through sediment starvation (Kidwell 1991). This is further suggested by the presence of *Rhizocorallium* traces, typical of firmground facies (Pemberton et al. 2004).

The second context for fossil concentrations is developed near the tops of two regionally traceable parasequences, where a shelly and slightly sandy facies (S3) is present. The lower of these occurs several meters above the fossiliferous concretions and is dominated almost to exclusion by *Liostrea strigilecula*. The other occurs several meters higher and is dominated by *Camptonectes bellistriatus*. In both of these parasequences, shells are preserved in a series of very thin to thin beds that coalesce into a single shell bed at the top of the parasequence, consistent with progressively slower sedimentation as a result of sediment bypass near the top of a parasequence (Kidwell, 1991).

The reasons behind the faunal distinctiveness of the Redwater fossil concentrations are unclear. Part of it may reflect changes in salinity through time, with the concretionary horizon being the most distal and possibly most open marine, with the scallop and oyster beds suggesting more restricted salinity. Whatever the cause, it must have regional extent, as the composition of these shell beds does not appear to vary, at least within the extent of the Bighorn Basin.

The faunal composition of the Sundance Formation changes abruptly at flooding surfaces and at sequence boundaries, as predicted by numerical models (Holland 1995, 2000). The changes at flooding surfaces primarily reflect the juxtaposition of different facies, and such changes would be expected given the differentiation of Sundance faunas among facies. The fauna of the Sundance Formation also changes abrupt across the J4 sequence boundary. This is shown well in the faunal ordination (Fig. 10), on which the faunas of the lower and upper Sundance separate cleanly, primarily along NMS axis 1. In many individual outcrops, some of the faunal change across the J4 sequence boundary stems from the merging of the transgressive surface with the sequence boundary, which juxtaposes offshore mudstone atop shallow-marine facies. The difference in faunas must reflect more than simply a facies shift, as offshore mudstone of the lower Sundance is dominated by *Gryphaea nebrascensis* whereas the same environment in the upper Sundance is dominated by *Pachyteuthis densus*. Furthermore, shallow-marine faunas also differ from the lower to the upper Sundance, most likely reflecting the switch from carbonate to siliciclastic deposition. Although it is difficult to place precise estimates on the duration of unconformities, Imlay (1982) indicated that the J4 unconformity likely spans much of the Callovian Stage, currently calibrated to be 2.6 million years long (Cohen et al. 2013). In contrast, the durations of the J3 and J5 unconformities are thought to be much shorter (Imlay 1982), and this is consistent with those unconformities displaying no obvious faunal change.

Occurrence of Vertebrate Fossils

In contrast to invertebrate fossils, the stratigraphic controls on the distribution of marine vertebrate fossils are less well understood. Many of the principles that control the distribution of invertebrates should also apply to marine vertebrates, but few field studies have tested this (Rogers and Kidwell 2000; Allulee and Holland 2005; Peters et al. 2009).

In a series of numerical models, three parameters are of particular importance for describing the stratigraphic occurrence of invertebrates (Holland 1995). Preferred environment is the environment, expressed by a depositional facies, in which a species is most likely to be found. Peak abundance is the probability of finding that species in that environment.

Environmental tolerance describes the degree to which the species occurs in other environments.

The combination of these three parameters describes how and the extent to which the stratigraphic record controls the fossil record. For example, when species have a limited environmental tolerance and a large peak abundance, their occurrence will appear to be strongly tied to depositional environment, often with the effect of pronounced changes in faunal composition across flooding surfaces and surfaces of forced regression. Likewise, large values of peak abundance will make changes in faunal composition across sequence-bounding unconformities more pronounced.

The extent to which marine vertebrates and invertebrates share similar patterns of stratigraphic occurrence will be controlled by the similarity of their values of preferred environment, peak abundance, and environmental tolerance. Differences in abundance are likely to cause patterns of occurrence to differ between marine vertebrates and invertebrates. The comparative rarity of marine vertebrates effectively raises the importance of sampling bias relative to facies bias and unconformity bias (Holland and Patzkowsky 1999) and as a result, the occurrence of vertebrates is more likely to appear stochastic and less controlled by facies and stratigraphic architecture than invertebrates.

It is also possible that differences in ecological needs may cause the distribution of marine vertebrates and invertebrates to differ. In both modern and ancient marine ecosystems, invertebrate ecology is strongly tied to factors that vary along depth gradients (see discussion in Holland 2000, and Patzkowsky and Holland 2012). This is true, not only for both attached and mobile benthic species, but also for swimming species, who may have ecological needs tied to the seafloor, such as preferred prey. Such a link between swimming species and the seafloor is seen in the close connection between ammonoid distributions and sedimentary facies (Scott 1940; Bayer and McGhee 1985). Some vertebrates show these strong connections to bathymetric zones, such as conodonts (e.g., Clark 1984) and fish (e.g., Connell and Lincoln-Smith 1999). Whether the ecology of marine vertebrates is generally tightly tied to the seafloor is unclear, and surface-feeding vertebrates almost certainly have a much weaker coupling to the seafloor. Finally, the propensity for large vertebrates to float for several weeks following death (Schäfer 1972) greatly increases the possibility for out-of-habitat transport that would weaken any relationship with sedimentary environment.

Marine invertebrate fossils can often be concentrated as a lag at an erosional surface, such as a sequence boundary or surface of forced regression. Similarly, bone is reliably found in the Sundance at the basal lag immediately overlying the J5 sequence boundary at the base of the Windy Hill Sandstone. As would be expected given the sedimentology of a lag deposit, bone at the J5 surface is always disarticulated and dissociated, and it is broken and highly abraded as well. Bone from this same context in the Cretaceous Judith River Formation of Montana (Rogers and Kidwell 2000; Rogers and Brady 2010) and the Eocene of Egypt (Peters et al. 2009) shows a similar style of preservation. Peters et al. (2009) found well-preserved bone within the falling-stage systems tract, but we did not find similar occurrences in the Sundance.

Concentrations of marine vertebrate skeletal material could also be expected at hiatal surfaces, such as condensed sections. In the Sundance, bone occurs in such a setting at the J5 maximum flooding surface, where invertebrates and bone are preserved in and associated with carbonate concretions. In the Sundance, this setting produces articulated ichthyosaurs (*Ophthalmosaurus natans*; Massare and Sperber 1999; Massare 2004; Massare et al. 2006) and partially articulated long-necked cryptocleidoid plesiosaurs (*Pantosaurus striatus*; O'Keefe and Wahl 2003; Wahl et al. 2007; O'Keefe et al. 2009). One indication of the reliability of finding bone at this setting came on our final day of field work. When we examined a new section exposing this interval, we found within one hour over 100 vertebrae, rib fragments, and gastralia of an ichthyosaur, as well as evidence of two vertebrate excavations nearby (Fig. 11C). Early studies of the Sundance recognized the importance of this interval, and Othniel Marsh (1891) called the concretionary interval the *Baptanodon* (now *Ophthalmosaurus*) beds. Similarly, Peters et al. (2009) found articulated whales at late TST flooding surfaces in the Eocene of Egypt.

Isolated articulated specimens are also found within the Sundance, unassociated with any significant surface. Offshore mudstone of the Redwater Shale has yielded the ichthyosaur *Ophthalmosaurus natans*, the plesiosaur *Pantosaurus striatus*, and the pliosaur *Megalneusaurus rex* (Wahl et al. 2007, 2010). Similarly, shoreface sandstone of the Redwater Shale has produced a partial skeleton of the long-necked cryptocleidoid plesiosaur *Tatenectes laramiensis* (O'Keefe and Street 2009; Street and O'Keefe 2010; O'Keefe et al. 2011).

As is true in the Cretaceous of Montana (Rogers and Kidwell 2000), flooding surfaces in the Sundance, where offshore successions overlie shoreface or shelly sandstone, did not produce bone. Peters et al. (2009) did find bone at some flooding surfaces, but primarily at maximum flooding surfaces. Allulee and Holland (2005) found concentrations of fish bone at flooding surfaces, but in most cases, these represented transgressive reworking of underlying bone-rich sediment, similar to what Rogers and Kidwell (2000) noted in the Cretaceous of Montana.

CONCLUSIONS

1. Along the eastern side of the Bighorn Basin in Wyoming, the Jurassic Sundance Formation consists of four depositional sequences. The lower two sequences are typically carbonate dominated, but some facies have terrigenous mudstone and quartz sand. The upper two sequences are primarily siliciclastic, but have several bioclastic horizons. Two horizons of incised valley fill are present; one is within the Hulett Member in the middle of the Sundance, and one is the Windy Hill Sandstone at the top of the Sundance. The unconformities recognized in this study agree well with previous regional studies.
2. Invertebrate fossils in the Sundance Formation follow well-established patterns of occurrence, with strong facies control of faunas, and concentrations of fossils in zones of low net sedimentation, such as at maximum flooding surfaces, the uppermost portions of some parasequences, and where an estuarine facies association overlies sequence-bounding unconformities.
3. Vertebrate fossils in the Sundance are represented primarily by ichthyosaurs, long-necked cryptocleidoid plesiosaurs, and pliosaurs. Owing to their comparative rarity, their patterns of occurrence are not as apparent as those of the invertebrates. Even so, vertebrates are primarily found in offshore mudstone, and to a lesser extent shoreface sandstone, of the siliciclastic Redwater Shale in the upper half of the Sundance. In addition, skeletal material is common near hiatal surfaces, including a zone of concretions at the maximum flooding surface in the Redwater Shale. Isolated highly degraded bone is also found in lag deposits where a tidal estuarine facies association overlies sequence-bounding unconformities. Such associations suggest that sequence stratigraphic architecture may be a useful tool for prospecting for vertebrate fossils, and that sequence stratigraphic context should be considered when interpreting marine vertebrate fossils.

ACKNOWLEDGMENTS

We thank Sean Cameron, Jon Primm, Brooke Hamil, and Ben Wilhelm for their assistance in the field and for discussions of Sundance stratigraphy. We also thank Cliff and Row Manuel for their hospitality, lodging, and help with locating outcrops. We are grateful to Dr. Glenn Storrs who helped with

contacts and preliminary field site locations. We also appreciate the access to collections granted by Michael Cassiliano at the University of Wyoming and the Thermopolis Dinosaur Center. We thank Bruce Railsback and Sally Walker for their helpful comments on an early version of this manuscript, and we thank the two anonymous PALAIOS reviewers and Associate Editor for their helpful comments. SKM thanks the Geological Society of America, the Paleontological Society, and the Miriam Watts-Wheeler Fund for generous financial support for this research. SMH appreciates the support of the University of Georgia Provost Summer Research Fund.

SUPPLEMENTAL MATERIAL

Data is available from the PALAIOS Data Archive: http://www.sepm.org/pages.aspx?pageid=332.

REFERENCES

Ahlbrandt, T.S., and Fox, J.E., 1997, Middle Jurassic incised valley fill (eolian/estuarine) and nearshore marine petroleum reservoirs, Powder River Basin: The Mountain Geologist, v. 34, p. 97–115.

Allulee, J.L., and Holland, S.M., 2005, The sequence stratigraphic and environmental context of primitive vertebrates: Harding Sandstone, Upper Ordovician, Colorado, USA: PALAIOS, v. 20, p. 518–533.

Andersson, K.A., 1979, Early lithification of limestones in the Redwater Shale Member of the Sundance Formation (Jurassic) of southeastern Wyoming: University of Wyoming Contributions to Geology, v. 18, p. 1–17.

Aurell, M., Bosence, D., and Waltham, D., 1995, Carbonate ramp depositional systems from a Late Jurassic epeiric platform (Iberian Basin, Spain): a combined computer modelling and outcrop analysis: Sedimentology, v. 42, p. 75–94.

Azeredo, A.C., 1998, Geometry and facies dynamics of Middle Jurassic carbonate ramp sandbodies, *in* Wright, V.P., and Burchette, T.P., 1998, Carbonate Ramps: Geological Society, London, Special Publications, v. 149, p. 281–314.

Bayer, U., and McGhee, G.R., 1985, Evolution in marginal epicontinental basins: the role of phylogenetic and ecologic factors (ammonite replacements in the German Lower and Middle Jurassic), *in* Bayer, U., and Seilacher, A., eds., Sedimentary and Evolutionary Cycles: New York, Springer-Verlag, p. 164–220.

Blake, D.B., 1981, The new Jurassic sea star genus *Eokainaster* and comments on life habits and the origins of the modern Asteroidea: Journal of Paleontology, v. 55, p. 33–46.

Blakey, R., 2013, North American paleogeographic maps, http://cpgeosystems.com/nam.html. Checked April 2013.

Brenner, R.L., and Davies, D.K., 1973, Storm-generated coquinoid sandstone: genesis of high-energy marine sediments from the Upper Jurassic of Wyoming and Montana: Geological Association of America Bulletin, v. 84, p. 1685–1698.

Brenner, R.L., and Davies, D.K., 1974, Oxfordian sedimentation in Western Interior United States: American Association of Petroleum Geologists Bulletin, v. 58, p. 407–428.

Brenner, R.L., Swift, D.J.P, and Gaynor, G.C., 1985, Reevaluation of coquinoid sandstone depositional model, Upper Jurassic of central Wyoming and south-central Montana: Sedimentology, v. 32, p. 363–372.

Brett, C., 1995, Sequence stratigraphy, biostratigraphy, and taphonomy in shallow marine environments: PALAIOS, v. 10, p. 597–616.

Burchette, T.P., and Wright, V.P., 1992, Carbonate ramp depositional systems: Sedimentary Geology, v. 79, p. 3–57.

Calloman, J.H., 1982, A review of the biostratigraphy of the post-lower Bajocian Jurassic ammonites of western and northern North America, *in* Westermann, G.E.G, ed., Jurassic–Cretaceous Biochronology and Paleogeography of North America: Geological Association of Canada, Special Paper 27, p. 143–174.

Clark, D.L., 1984, Conodont biofacies and provincialism: Geological Society of America Special Paper, v. 196, p. 1–340.

Clark, N.D.L., and Brett-Surman, M.K., 2008, A comparison between dinosaur footprints from the Middle Jurassic of the Isle of Skye, Scotland, UK, and Shell, Wyoming, USA: Scottish Journal of Geology, v. 44, p. 139–150.

Clifton, H.E., 2006, A reexamination of facies models for clastic shorelines: SEPM Special Publication, v. 84, p. 293–337.

Cohen, K.M., Finney, S.C., Gibbard, P.L., and Fan, J.X., 2013, The ICS international stratigraphic chart: Episodes, v. 36, p. 199–204.

Connell, S.D., and Lincoln-Smith, M.P., 1999, Depth and the structure of assemblages of demersal fish: experimental trawling along a temperate coast: Estuarine, Coastal and Shelf Science, v. 48, p. 483–495.

Connely, M.V., 2006, Paleoecology of pterosaur tracks from the Upper Sundance and Lower Morrison Formations in central Wyoming: New Mexico Museum of Natural History and Science Bulletin, v. 36, p. 199–202.

DeCelles, P.G., 2004, Late Jurassic to Eocene evolution of the Cordilleran thrust belt and foreland basin system, western U.S.A.: American Journal of Science, v. 304, p. 105–168.

DeCelles, P.G., and Currie, B.S., 1996, Long-term sediment accumulation in the Middle Jurassic: early Eocene Cordilleran retroarc foreland basin system: Geology, v. 24, p. 591–594.

DeJarnette, M.L., and Utgaard, J.E., 1986, Facies and depositional environments of a mixed carbonate-clastic sequence in the Sundance Formation (Jurassic), northeastern Bighorn Basin, Montana and Wyoming: geology of the Beartooth Uplift and adjacent basins: Montana Geological Society and Yellowstone Bighorn Research Association Joint Field Conference and Symposium, v. 1, p. 27–31.

Dunham, R.J., 1962, Classification of carbonate rocks according to depositional texture, *in* Ham, W.E., ed., Classification of Carbonate Rocks, American Association of Petroleum Geologists Memoir, v. 1, p. 108–121.

Eberth, D.A., Brinkman, D.B., Chen, P.J., Yuan, F.T., Wu, S.Z., Li, G., and Cheng, X.S., 2001, Sequence stratigraphy, paleoclimate patterns, and vertebrate fossil preservation in Jurassic–Cretaceous strata of the Junggar Basin, Xingjiang Autonomous Region, People's Republic of China: Canadian Journal of Earth Sciences, v. 38, p. 1627–1644.

Fuentes, F., DeCelles, P.G., and Gehrels, G.E., 2009, Jurassic onset of foreland basin deposition in northwestern Montana, USA: Implications for along-strike synchroneity of Cordilleran orogenic activity: Geology, v. 37, p. 379–382.

Fürsich, F.T., and Heinberge, C., 1983, Sedimentology, biostratinomy, and palaeoecology of an Upper Jurassic offshore sand bar complex: Bulletin of the Geologic Society of Denmark, v. 32, p. 67–95.

Fürsich, F.T., Freytag, S., Röhl, J., and Schmid, A., 1995, Palaeoecology of benthic associations in salinity-controlled marginal marine environments: Examples from the lower Bathonian (Jurassic) of the Causses (southern France): Palaeogeography, Palaeoclimatology, Palaeoecology, v. 113, p. 135–172.

Harris, J., and Lacovara, K., 2004, Enigmatic fossil footprints from the Sundance Formation (Upper Jurassic) of Bighorn Canyon National Recreation Area, Wyoming: Ichnos, v. 11, p. 151–166.

Heller, P. L., Bowdler, S. S., Chambers, H. P., Coogan, J. C., Hagen, E. S., Shuster, M. W., Winslow, N. S., and Lawton, T. F., 1986, Time of initial thrusting in the Sevier orogenic belt, Idaho-Wyoming and Utah: Geology, v. 14, p. 388–391.

Herrick, E.M., and Schram, F.R., 1978, Malacostracan crustacean fauna from the Sundance Formation (Jurassic) of Wyoming: American Museum Novitates, v. 2652, p. 1–12.

Holland, S.M., 1995, The stratigraphic distribution of fossils: Paleobiology, v. 21, p. 92–109.

Holland, S.M., 2000, The quality of the fossil record: A sequence stratigraphic perspective: PALAIOS, v. 26, p. 148–168.

Holland, S.M., and Patzkowsky, M.E., 1999, Models for simulating the fossil record: Geology, v. 27, p. 491–494.

Howard, J.D., Frey, R.W., and Reineck, H.E., 1972, Georgia coastal region, Sapelo Island, U.S.A.: Sedimentology and Biology, I, v. 4, p. 3–14.

Hunter, A.W., and Zonneveld, J.P., 2008, Palaeoecology of Jurassic encrinites: reconstructing crinoid communities from the Western Interior Seaway of North America: Palaeogeography, Palaeoclimatology, Palaeoecology, v. 263, p. 58–70.

Imlay, R.W., 1947, Marine Jurassic of the Black Hills area, South Dakota and Wyoming: American Association of Petroleum Geologists Bulletin, v. 31, p. 227–273.

Imlay, R.W., 1948, Characteristic marine Jurassic fossils from the western interior of the United States: U.S. Geological Survey Professional Paper 214-B, p. 13–33.

Imlay, R.W., 1956, Marine Jurassic exposed in Bighorn Basin, Pryor Mountains, and northern Bighorn Mountains, Wyoming and Montana: American Association of Petroleum Geologist Bulletin, v. 40, p. 562–599.

Imlay, R.W., 1957, Paleoecology of Jurassic seas in the Western Interior of the United States: Geological Society of America Memoir, v. 67, p. 469–599.

Imlay, R.W., 1962, Correlation of the Jurassic formations of North America, exclusive of Canada: Bulletin of the Geological Society of America, v. 65, p. 953–992.

Imlay, R.W., 1965, Jurassic marine faunal differentiation in North America: Journal of Paleontology, v. 39, p. 1023–1038.

Imlay, R.W., 1980, Jurassic paleobiogeography of the conterminous United States in its continental setting: U.S. Geological Survey Professional Paper, v. 1062, p. 1–141.

Imlay, R.W., 1982, Jurassic (Oxfordian and late Callovian) ammonites from the Western Interior region of the United States: U.S. Geological Survey Professional Paper 1232, 44 p.

Ingram, R.L., 1954, Terminology for thickness of stratification and parting units in sedimentary rocks: Geological Society of America Bulletin, v. 65, p. 937–938.

Johnson, E.A., 1992, Depositional history of Jurassic rocks in the area of the Powder River Basin, northeastern Wyoming and southeastern Montana: U.S. Geological Survey Bulletin 1917-J, 38 p.

Kidwell, S.M., 1991, The stratigraphy of shell concentrations, *in* Allison, P.A., and Brings, D.E.G., eds., Taphonomy: Releasing the Data Locked in the Fossil Record: New York, Plenum, p. 211–290.

Kilibarda, Z., and Loope, D.B., 1997, Jurassic Aeolian oolite on paleohigh in the Sundance Sea, Bighorn Basin, Wyoming: Sedimentology, v. 44, p. 391–404.

Kocurek, G., and Dott, R.H., 1983, Jurassic paleogeography and paleoclimate of the central and southern Rocky Mountains region, *in* Reynolds, M.W., and Dolly, E.D., eds., Mesozoic Paleogeography of the West-Central United States: Rocky Mountain Section, Society of Economic Paleontologists and Mineralogists, Rocky Mountain Paleogeography Symposium no. 2. Denver, Colorado, USA, p. 101–16.

Kowallis, B.J., Christiansen, E.H., Deino, A.L., Peterson, F., Turner, C.E., Kunk, M.J., and Obradovich, J.D., 1998, The age of the Morrison Formation: Modern Geology, v. 22, p. 235–260.

Kreisa, R.D., and Moiola, R.J., 1986, Sigmoidal tidal bundles and other tide-generated sedimentary structures of the Curtis Formation, Utah: Geological Society of America Bulletin, v. 97, p. 381–387.

Kvale, E.P, Johnson, G.D., Mickelson, D.L., Keller, K., Furer, L.C., and Archer, A.W., 2001, Middle Jurassic (Bajocian and Bathonian) dinosaur megatracksites, Bighorn Basin, Wyoming, U.S.A.: PALAIOS, v. 16, p. 233–254.

Kvale, E., Mickelson, D., Hasiotis, S.T., and Johnson, G., 2004, The history of dinosaur footprint discoveries in Wyoming with emphasis on the Bighorn Basin: Ichnos, v. 11, p. 3–9.

Legendre, P., and Legendre, L., 1998, Numerical Ecology, 2nd English edition: Amsterdam, Elsevier, 853 p.

Lockley, M.G., and Wright, J.L, 2003, Pterosaur swim tracks and other ichnological evidence of behaviour and ecology: Geological Society of London Special Publications, v. 217, p. 297–313.

Logue, T.J., 1977, Preliminary investigations of pterodactyl footprints at Alcova, Wyoming: Wyoming Geological Association, Earth Science Bulletin, v. 10, p. 29–30.

Loughney, K.M., Fastovsky, D.E., and Parker, W.G., 2011, Vertebrate fossil preservation in blue paleosols from the Petrified Forest National Park, Arizona, with implications for vertebrate biostratigraphy in the Chinle Formation: PALAIOS, v. 26, p. 700–719.

Marsh, O.C., 1891, Geological horizons as determined by vertebrate fossils: American Journal of Science, v. 42, p. 336–338.

Massare, J.A., 2004, Ichthyosaur diversity in the upper Sundance Formation (Jurassic, Oxfordian), Wyoming: Journal of Vertebrate Paleontology, v. 24, issue 3 supplement, p. 90.

Massare, J.A., and Sperber, S., 1999, Taphonomy of an ichthyosaur from the Jurassic Sundance Formation: Journal of Vertebrate Paleontology, v. 19, issue 3 supplement, p. 62.

Massare, J.A., Buchholtz, E.A., Kenney, J.M., and Chomat, A.M., 2006, Vertebral morphology of *Ophthalmosaurus natans* (Reptilia: Ichthyosauria) from the Jurassic Sundance Formation of Wyoming: Paludicola, v. 5, p. 242–254.

Massare, J.A., Wahl, W.R., Ross, M., and Connely, M.V., 2014, Palaeoecology of the marine reptiles of the Redwater Shale Member of the Sundance Formation (Jurassic) of central Wyoming, USA: Geological Magazine, v. 151, p. 167–182.

McCune, B., and Grace, J.B., 2002, Analysis of Ecological Communities: MjM Software Design, Gleneden Beach, Oregon, 300 p.

Miall, A.D., 2009, Initiation of the Western Interior foreland basin: Geology, v. 37, p. 383–384.

Mickelson, D.L., Mickelson, K.A., King, M.R., and Getty, P., 2006, Jurassic dinosaur tracksites from the American West: New Mexico Museum of Natural History and Science Bulletin, v. 34, p. 138–140.

O'Keefe, F.R., and Street, H.P., 2009, Osteology of the cryptocleidoid plesiosaur *Tatenectes laramiensis*, with comments on the taxonomic status of the Cimolisauridae: Journal of Vertebrate Paleontology, v. 29, p. 48–57.

O'Keefe, F.R., and Wahl, W., 2003, Current taxonomic status of the plesiosaur *Pantosaurus striatus* from the Upper Jurassic Sundance Formation, Wyoming: Paludicola, v. 4, p. 37–46.

O'Keefe, F.R., Street, H.P., Cavigelli, P., Socha, J.J., and O'Keefe, D.R., 2009, A plesiosaur containing an ichthyosaur embryo as stomach contents from the Sundance Formation of the Bighorn Basin, Wyoming: Journal of Vertebrate Paleontology, v. 29, p. 1306–1310.

O'Keefe, F.R., Street, H.P., Wilhelm, B.C., Richards, C., and Zhu, H., 2011, A new skeleton of the cryptoclidid plesiosaur *Tatenectes laramiensis* reveals a novel body shape among plesiosaurs: Journal of Vertebrate Paleontology, v. 31, p. 330–339.

Palmer, C.P., Boyd, D.W., and Yochelson, E.L., 2004, The Wyoming Jurassic fossil *Dentalium subquadratum* Meek, 1860 is not a scaphopod but a serpulid worm tube: Rocky Mountain Geology, v. 39, p. 85–91.

Parcell, W.C., and Williams, M.K., 2005, Mixed sediment deposition in a retro-arc foreland basin: Lower Ellis Group (M. Jurassic), Wyoming and Montana, U.S.A.: Sedimentary Geology, v. 177, p. 175–194.

Patzkowsky, M.E., and Holland, S.M., 2012, Stratigraphic Paleobiology: University of Chicago Press, 256 p.

Pemberton, S.G., MacEachern, J.A., and Saunders, T.D., 2004, Stratigraphic applications of substrate-specific ichnofacies: delineating discontinuities in the rock record, *in* McIlroy, D., ed., The application of ichnology to palaeoenvironmental and stratigraphic analysis: London, Geological Society of London Special Publication 228, p. 29–62.

Peters, S., Sameh, M., Zalmout, I., and Gingerich, P., 2009, Sequence stratigraphic control on preservation of late Eocene whales and other vertebrates at Wadi Al-Hitan, Egypt: PALAIOS, v. 24, p. 290–302.

Peterson, J.A., 1954, Jurassic ostracoda from the "lower" Sundance and Rierdon Formations, Western Interior United States: Journal of Paleontology, v. 28, p. 153–176.

Peterson, F., 1994, Sand dunes, sabkhas, streams, and shallow seas: Jurassic paleogeography in the southern part of the Western Interior Basin, *in* Caputo, M.V., Peterson, J.A., and Franczyk, K.J., eds., Mesozoic Systems of the Rocky Mountain Region, USA: Rocky Mountain Section, Society of Economic Paleontologists and Mineralogists, Denver, Colorado, p. 233–272.

Pettijohn, F.J., Potter, P.E., and Siever, R., 1987, Sand and Sandstone, 2nd ed.: New York, Springer-Verlag, 553 p.

Pipiringos, G.N., 1968, Correlation and nomenclature of some Triassic and Jurassic rocks in south-central Wyoming: U.S. Geological Survey Professional Paper, v. 594-D, p. 1–25.

Pipiringos, G.N., and O'Sullivan, R.B., 1978, Principal unconformities in Triassic and Jurassic rocks, Western Interior United States: a preliminary survey: U.S. Geological Survey Professional Paper, v. 1035-A, p. 29.

R Development Core Team, 2011, R: a language and environment for statistical computing, Version 2.11.1: Vienna, R Foundation for Statistical Computing.

Raaf, J.M.F., and Van Gelder, A., 1977, Wave-generated structures and sequences from a shallow marine succession, lower Carboniferous, County Cork, Ireland: Sedimentology, v. 24, p. 451–483.

Rautman, C.A., 1978, Sedimentology of Late Jurassic barrier-island complex: lower Sundance Formation of Black Hills: American Association of Petroleum Geologists Bulletin, v. 62, p. 2275–2289.

Rogers, R.R., and Brady, M.E., 2010, Origins of microfossil bonebeds: insights from the Upper Cretaceous Judith River Formation of north-central Montana: Paleobiology, v. 36, p. 80–112.

Rogers, R.R., and Kidwell, S.M., 2000, Associations of vertebrate skeletal concentrations and discontinuity surfaces in terrestrial and shallow marine records: A test in the Cretaceous of Montana: The Journal of Geology, v. 108, p. 131–154.

Santiago-Blay, J.A., Labandeira, C.C., Pribyl, L., Hotton, C., and Martin, L.D., 2001, The Sundance insect fauna (Middle Jurassic) of northern Wyoming and southern Montana: Geological Society of America Abstracts with Programs, v. 33, p. 266.

Schäfer, W., 1972, Ecology and palaeoecology of marine environments: University of Chicago Press, 568 p.

Schmude, D.E., 2000, Interplay of paleostructure, sedimentation and preservation of Middle Jurassic rocks, Bighorn Basin, Wyoming: The Mountain Geologist, v. 37, p. 145–155.

Schultze, H.P., and Enciso, G., 1983, Middle Jurassic age of the fish-bearing horizon in the Cañon City Embayment, Colorado: Journal of Paleontology, v. 57, p. 1053–1060.

Scott, G., 1940, Paleoecological factors controlling the distribution and mode of life of Cretaceous ammonoids in the Texas area: Journal of Paleontology, v. 14, p. 299–323.

Shanley, K.W., McCabe, P.J., and Hettinger, R.D., 1992, Tidal influence in Cretaceous fluvial strata from Utah, USA: a key to sequence stratigraphic interpretation: Sedimentology, v. 39, p. 905–930.

Specht, R.W., and Brenner, R.L., 1979, Storm-wave genesis of bioclastic carbonates in Upper Jurassic epicontinental mudstones, east-central Wyoming: Journal of Sedimentary Petrology, v. 49, p. 1307–1322.

Stone, R., and Vondra, C.F., 1972, Sediment dispersal patterns of oolitic calcarenite in the Sundance Formation (Jurassic), Wyoming: Journal of Sedimentary Petrology, v. 42, p. 227–229.

Street, H.P., and O'Keefe, F.R., 2010, Evidence of pachyostosis in the cryptocleidoid plesiosaur *Tatenectes laramiensis* from the Sundance Formation of Wyoming: Journal of Vertebrate Paleontology, v. 30, p. 1279–1282.

Swain, F.M., and Peterson, J.A., 1952, Ostracodes from the upper part of the Sundance Formation of South Dakota, Wyoming and Southern Montana: U.S. Geological Survey Professional Paper, v. 243-A, p. 1–31.

Uhlir, D.M., Akers, A., and Vondra, C.F., 1988, Tidal inlet sequence, Sundance Formation (Upper Jurassic), north-central Wyoming: Sedimentology, v. 35, p. 739–752.

Wahl, W.R., 1998, Plesiosaur gastric contents from the upper Redwater Shale (lower Oxfordian) of the Sundance Formation (Jurassic) of Wyoming: Journal of Vertebrate Paleontology, v. 18, issue 3 supplement, p. 84.

Wahl, W.R., 2008, Decapod material associated with ichthyosaur remains from the Sundance Formation of Natrona County, Wyoming: Geological Society of America Abstracts with Program, v. 40, p. 41.

Wahl, W.R., 2009, Taphonomy of a nose dive: bone and tooth displacement and mineral accretion in an ichthyosaur skull: Paludicola, v. 7, p. 107–116.

Wahl, W.R., Ross, M., and Massare, J.A., 2007, Rediscovery of Wilbur Knight's *Megalneusaurus rex* site: new material from an old pit: Paludicola, v. 6, p. 94–104.

Wahl, W.R., Massare, J.A., and Ross, M., 2010, New material from the type specimen of *Megalneusaurus rex* (Reptilia: Sauropterygia) from the Jurassic Sundance Formation, Wyoming: Paludicola, v. 7, p. 170–180.

West, C.M., 1985, Stratigraphy and depositional environments of the lower Sundance Formation, eastern Bighorn Basin, Wyoming: Unpublished M.S. thesis, University of Wyoming, Laramie, 94 p.

Wilhelm, B.C., and O'Keefe, F.R., 2010, A new partial skeleton of a cryptocleidoid plesiosaur from the Upper Jurassic Sundance Formation of Wyoming: Journal of Vertebrate Paleontology, v. 30, p. 1736–1742.

Wright, R.P., 1973, Marine Jurassic of Wyoming and South Dakota: its paleoenvironments and paleobiogeography: University of Michigan Museum of Paleontology Papers on Paleontology, v. 2, p. 49.

Wright, R.P., 1974, Jurassic bivalves from Wyoming and South Dakota: a study of feeding relationships: Journal of Paleontology, v. 48, p. 425–433.

Submitted 10 December 2013; accepted 2 June 2014.